ASSESSMENT OF URANIUM-FREE NITRIDE FUELS FOR SPENT FUEL TRANSMUTATION IN FAST REACTOR SYSTEMS

A Thesis

by

FRANK JOSEPH SZAKALY

Submitted to the Office of Graduate Studies of
Texas A&M University
in partial fulfillment of the requirements for the degree of

MASTER OF SCIENCE

May 2004

Major Subject: Nuclear Engineering

ASSESSMENT OF URANIUM-FREE NITRIDE FUELS FOR SPENT FUEL TRANSMUTATION IN FAST REACTOR SYSTEMS

A Thesis

by

FRANK JOSEPH SZAKALY

Submitted to Texas A&M University
in partial fulfillment of the requirements
for the degree of

MASTER OF SCIENCE

Approved as to style and content by:

_____	_____
Kenneth L. Peddicord (Chair of Committee)	K. Ted Hartwig (Member)
_____	_____
Marvin L. Adams (Member)	William E. Burchill (Head of Department)

May 2004

Major Subject: Nuclear Engineering

ABSTRACT

Assessment of Uranium-free Nitride Fuels for Spent Fuel

Transmutation in Fast Reactor Systems. (May 2004)

Frank Joseph Szakaly, B.A., University of Rochester

Chair of Advisory Committee: Dr. Kenneth L. Peddicord

The purpose of this work is to investigate the implementation of nitride fuels containing little or no uranium in a fast-spectrum nuclear reactor to reduce the amount of plutonium and minor actinides in spent nuclear fuel destined for the Yucca Mountain Repository. A two tier recycling strategy is proposed. Thermal spectrum transmutation systems converted from the existing LWR fleet were modeled for the first tier, and the Japanese fast reactor MONJU was used for the fast-spectrum transmutation. The modeling was performed with the Monteburns code.

Transmutation performance was investigated as well as delayed neutron fraction, heat generation rates, and radioactivity of the spent material in the short and long term for the different transmutation fuel cycles. A two-tier recycling strategy incorporating fast and thermal transmutation with uranium-free nitride fuel was shown to reduce the long-term heat generation rates and radioactivity of the spent nuclear fuel inventory.

ACKNOWLEDGEMENTS

I'd like to thank my advisor Dr. Peddicord for his help and support, and also I'd like to thank the Texas A&M Nuclear Engineering Department faculty and staff. In addition I would like to thank Dr. Hartwig of the Mechanical Engineering Department and Dr. Adams from the Nuclear Engineering Department for serving on my committee.

Special thanks go to the Department of Energy's Office of Nuclear Energy, Science and Technology. I am very grateful to have received from them an Advanced Fuel Cycle Initiative fellowship, which has provided me with the inspiration for this project and the funding to accomplish it. I would also like to thank the University Research Alliance and all the very helpful people who work there, and the Department of Energy and the various labs of theirs I've worked in: Oak Ridge National Laboratory and Los Alamos National Laboratory.

In addition I would like to thank Dr. William Charlton from Texas A&M University and Dr. Hiroshi Nishi of the Japan Nuclear Cycle Development Institute (JNC), who really helped me get my research to work with their invaluable time, guidance, patience and knowledge.

I would also like to acknowledge my parents: thank you for everything you've given to me and done for me, and all of my friends, from Baldwinsville, Rochester, Texas and everywhere in between.

Finally and most of all, I'd like to thank Chrissy Polyn for everything she has given to me. I love you for always, Chrissy.

TABLE OF CONTENTS

CHAPTER Page

LIST OF FIGURES

Page

Page

Page

LIST OF TABLES

Page

CHAPTER I

INTRODUCTION

Introduction

The issue of spent fuel transmutation is a complicated one both scientifically and politically. After many years of neglect in the United States, this topic is at the forefront of the many issues concerning the Department of Energy. The statutory limit on the size of the recently approved Yucca Mountain Repository (YMR) is 70,000 tonnes of material, 63,000 of which are available for commercial reactor fuel, the remainder being reserved for military use. The US reactors are currently producing 2,000 tonnes of spent fuel per year. This is noteworthy, since the total estimate for the amount of spent fuel we will have in the United States at the end of the licensing periods of all reactors currently operating is already more than the capacity of YMR at 87,000 tonnes [1]. Regardless of the talk about potentially extending the Yucca Mountain license, clearly the issue of transmutation needs to be addressed to reduce the spent nuclear fuel inventory, as the probability of finding another repository site and characterizing it completely, and in a reasonable amount of time, would be expected to be difficult. The anticipated cost of a second repository is ~$50 billion, and YMR itself took 20 years to characterize and approve [2]. In addition, it is important to note that the vast majority of material in spent fuel is not simply radioactive "waste," but useful nuclear fuel.

This thesis follows the style and format of the Journal of Nuclear Materials.

As a result, economically it seems unwise to simply put the spent fuel into Yucca Mountain without exploiting the energy reserves contained within the spent fuel, and it also seems unwise to consider a once-through fuel cycle that will continue filling up repositories. Such a strategy would eliminate the viability of nuclear power as a sustainable energy source.

Reprocessing and recycling of spent fuel has been a taboo subject in America since the 1970's and as a result, our technology and development in this area needs to be improved and expanded in the very near future. The Department of Energy is studying this under the Advanced Fuel Cycle Initiative (AFCI) program, which funded this study as part of the University Fellowship program. There are many issues to be addressed in the arena of spent fuel recycling and reprocessing: separations technology, fuel fabrication and development, repository design and modeling, and determination of the heat load and radiotoxicities of the waste stream (and how to reduce them), etc. In addition, the transmutation systems in which to use these fuels need to be determined. This study will consider only the ultimate burnup of the actinides, since with their long half lives these nuclides provide most of the burden in the long term for a repository. Both thermal and fast systems will be modeled, because although plutonium can be transmuted in a thermal spectrum light-water reactor, to effectively transmute minor actinides, a fast spectrum is required [3].

DOE Recycling Strategy

Now that the Department of Energy is considering reprocessing and recycling of spent nuclear fuel, there are many ideas of how transmutation of the spent fuel should be

accomplished. The current DOE plan is to use two tiers of recycling for the spent fuel. The Series I fuels are a modified mixed-oxide (MOX) fuel consisting of reprocessed uranium, plutonium and neptunium oxides for burning in existing LWR's. While there is a large database on this fuel form (MOX has been extensively tested and used in Europe commercially), one issue with it is that even upon multiple recycle, in a thermal reactor or a fast reactor, the use of MOX breeds in more americium and curium (even though much of the ^{239}Pu and ^{241}Pu is burned) [3].

The addition of neptunium is a possibility, and while studies are ongoing concerning the effects of this addition, it is assumed to be similar enough to commercial MOX to be used feasibly and without too many problems/differences [4]. In addition, for the long-term, neptunium can also aid in extending burnup in LWR's by producing plutonium, due to ^{237}Np's 150 barn neutron capture (n,γ) cross section for reaction 1.1a and ^{238}Pu's 540 barn (n,γ) cross section for reaction 1.1b [5].

$$^{237}Np + n \xrightarrow{150\ \text{barns}} {}^{238}Np + \gamma \xrightarrow{2.1\ \text{days}} {}^{238}Pu + \beta^{-} \qquad (1.1a)$$

$$^{238}Pu + n \xrightarrow{540\ \text{barns}} {}^{239}Pu + \gamma \qquad (1.1b)$$

Series II Fuels and Transmutation System

The choice for the Series II fuels is still to be determined, mostly because there is a very limited database on all the candidate fuel forms (metal, nitride, TRISO) and extensive testing is required, and currently being planned. This study, as stated before, models both fertile and fertile-free nitride fuels containing no or very small amounts of uranium, using instead thorium in the fertile fuel pins.

The Series II fuels will require a fast spectrum system for sufficient transmutation: both accelerator-driven systems and fast reactor systems are still being considered to transmute the minor actinides (MAs) [6]. Fast reactors are a proven technology that have been built all over the world and operated successfully. In addition, fast reactors have the additional advantage of possibly being integrated with the Generation IV reactor concepts, many of which are fast or epithermal designs. Accelerator-driven systems, on the other hand, are operated sub-critically and thus the safety issues (lower delayed neutron fraction, positive sodium reactivity void worth, etc) that arise with fast reactors (and which are likely worse with fertile-free transmutation fuels) can be somewhat mitigated. However, for this study we have chosen the Japanese Nuclear Commission's MONJU fast reactor as the Series II transmutation system.

While equilibrium and a closed fuel cycle is a long term goal, it bears remembering that the current stocks of spent LWR fuel need to be transmuted as well. Therefore this study looks at maximizing the plutonium and minor actinide transmutation, with a focus on reducing the inventory of these isotopes rather than attaining equilibrium. The idea of a closed fuel cycle in which the number of transmutation systems can balance the waste production from all of the commercial reactors in the United States is important and will be addressed but is somewhat beyond the scope of this study.

Nitride Fuels

The choice of nitride fuels is a logical one: nitride fuels have support in the DOE's AFCI program, and were chosen for this study because they also have many

beneficial attributes that make them potentially preferable to oxides. For example, as a transmutation fuel, nitrides have the benefit of being mostly mononitride compounds (PuN, AmN) as opposed to dioxide compounds (the more traditional UO_2 and PuO_2 currently being used) which means that there is a higher heavy metal density per mass unit of fuel. Another reason is that nitride fuel has a much better thermal conductivity than oxide fuel. Therefore, since the conductivity is higher, with a nitride-fueled core it should be possible to operate the reactor with a lower fuel temperature [7]. This is important because not only could the reactor core then be run at a higher power density, but also because of safety due to the fact that nitride fuels have the possibility of dissociating at temperatures below the melting point. Nitride fuels have also demonstrated very low fission gas release, which could help in extending the fuels to higher burnups [8].

However, one issue concerning the production of nitride fuels is important to discuss: standard ^{14}N should not be used to make nitride fuel for reactors, because it results in radioactive ^{14}C from its (n,p) reaction. Therefore, ^{15}N needs to be used when fabricating these fuels, which is more difficult to obtain, since natural nitrogen is 99.63% ^{14}N and only 0.37% ^{15}N, and thus more expensive [9]. However, according to Wallenius and Pillon, the cost should not be prohibitive, especially on a large scale, and the advantages to be gained from the positive characteristics of nitride fuel could far outweigh this drawback [10].

Thorium

In addition, the other reason this study is being undertaken is to replace the uranium in the transmutation fuel form with "something else". This "something else" can be one or more of many materials: inert matrix fuels, where the low-fertile fuel is mixed with zirconium nitride (ZrN) or with neutronically inert, high-temperature ceramics such as MgO, or a different fertile material, such as thorium [11]. By reducing or eliminating the fertile component (usually ^{238}U for uranium-fueled reactors) of the fuel to avoid breeding in more plutonium and minor actinides. Unfortunately, one of the problems both related to safety and performance with low-fertile and non-fertile fuels is this lack of fertile fuel in the core. For example, inert matrix fuels are a good option for the task of plutonium and minor actinide burning both in PWR's and in fast systems. However, a core made of inert matrix fuel raises some safety issues, such as a very low delayed neutron fraction. This means that a whole core loading cannot be used, and in a fast reactor system it would be even harder to control. In addition, inert-matrix fuels without fertile material present a greater reactivity swing over burnup which makes core management more difficult: there is a large excess reactivity in the beginning of the cycle from the inert-matrix assemblies but then at the end of life the reactivity has decreased so much that more power is required from the standard assemblies, and this also creates greater power peaks over core life [12].

The main issue with fertile material is that other materials will be bred into the reactor: if thorium is used then ^{232}U, ^{233}U and all their daughter isotopes will be created. This could help reactor performance by providing fissile material to extend burnup and

flatten the reactivity swing over the fuel cycle, or it could provide only proliferation concerns from the highly fissile ^{233}U. As far as the radiotoxicity of the fuel, it could prove to be even worse than the currently-used $^{235}U/^{238}U$ cycle. Putting thorium in the reactor will create ^{232}U, which decays to ^{212}Bi and ^{208}Tl, which decay with 727 keV and 2.614 MeV gammas, respectively. While this provides some proliferation protection, it also raises reprocessing and handling problems. This will be addressed in later chapters where the resulting products of this fuel cycle will be analyzed in detail [13,14].

Thorium has provided some positive results as well. In a thermal reactor model using oxide fuel, thorium was used as the fertile diluent for plutonium and fuel performance, plutonium incineration and reactor physics/safety parameters were improved as compared to inert matrix fuel options, and ~85% of the initial plutonium was burned using $(Th,Pu)O_2$, with a thorium concentration of 30% ThO_2 [12]. In addition, thorium has a history of actual use in real reactors and not just modeling studies: it has been burned in the Shippingsport PWR, as well as in the Fort St. Vrain HTGR, with fairly good results and very long burnups [15]. In addition, there is more thorium than uranium in the earth's crust and while economically uranium is preferable, it is possible that in the future thorium fuel cycles could become a means of hopefully providing not only a closed fuel cycle but a sustainable energy source for many years to come [16]. This study aims to provide some backup for the applicability of this candidate fuel to the purpose described above: primarily as a transmutation fuel but hopefully as a component in a closed fuel cycle.

Organization and Goals

The application of this thesis to the goals of the AFCI program and the field of spent fuel transmutation in general is to see the effects of using uranium-free and nearly uranium-free nitride fuels to minimize the production of plutonium and higher actinides bred in during the Series II stage of the transmutation fuel cycle. The Series I fuels will be modeled to provide the feed material for the Series II stage and to see if the fuel cycle can achieve some sort of equilibrium and be at least partially closed through this method.

The goals of this study are: 1.) To determine the atomic composition of reprocessed spent fuel which, when made into a nitride fuel form for transmutation in a fast reactor, gives the most effective burnup of plutonium and the higher actinides, after taking most the uranium out and replacing it with thorium, 2.) To calculate the burnup and see what waste results from the use of the semi-thorium fuel cycle, 3.) To determine the most transmutation-effective core arrangement of transmutation fuel pins and fresh fuel pins, and 4.) To see if the fuel cycle can be closed through this approach by linking the Series I and Series II fuel studies iteratively.

First, the procedure and methods of the work undertaken will be described in detail, and the Series I fuel calculations and results will be summarized (Ch.2). The Series II fuels results are discussed in Chapter 3. The attempts to link the two together and close the fuel cycle are given in Chapter 4. Finally, the conclusions that have been reached from the results of this study will be given in Chapter 5.

CHAPTER II

SERIES I FUEL CALCULATIONS AND RESULTS

Introduction

The Series I system, according to the approach currently envisioned by DOE, includes utilization of thermal spectrum light water reactors (the commercial reactors in the US currently operating are exclusively thermal spectrum light water reactors) in which some fraction of the fuel will be replaced with MOX (mixed-oxide fuel) to burn excess plutonium. The modeling method will be discussed first, and then the Series I transmutation system are described. Then, the results for various Series I fuel options at the pin level are described, and then the whole-core simulations. Finally, conclusions about the impact of this work on the fuel cycle are outlined.

Modeling Method

First, however, we need a discussion of the method used in modeling these fuels. The method used to model all the fuels and reactor systems, thermal and fast, in this study is the code Monteburns, which is a code from Los Alamos National Laboratory written to perform, as its name suggests, Monte Carlo burnup/depletion calculations. It utilizes a Perl script that links and iteratively runs two standard and widely available nuclear engineering codes, MCNP and ORIGEN.

MCNP is an industry-standard Monte Carlo code for general, user-defined geometries, developed at Los Alamos National Laboratory [17]. It has been thoroughly

tested and benchmarked, and is used by many people. MCNP version 5 was used for this study.

ORIGEN stands for Oak Ridge Isotope GENeration and Depletion code, which was, as its name suggests, developed at Oak Ridge National Laboratory in the early 1980's. The latest revision, Version 2.2, of ORIGEN was used for this work, which has a few advantages over ORIGEN2.1, the most important of which is modifications to the code to be able to more accurately predict the products of materials with a high minor actinide fraction (since our main objective is to burn minor actinides). The older version had problems correctly predicting the fission product yield from the higher actinides, but this has been resolved by using the new code and by decreasing the length of time steps to less than 100 days for materials containing a high fraction of minor actinides [18,19].

The Monteburns code runs MCNP to get flux information for each material, which it then uses to write an ORIGEN file and determine burnup of the materials over the time step. This data is then used to update the MCNP material concentrations for that time step, and then the program runs MCNP for the next time step with the updated information. The user can define which materials to track, how accurately to follow them, how long the time steps are (and how many to do), and what feed of new material there is in any region of the model, if any. It is a very flexible code, combining the ease of MCNP geometry specification and flux calculation with the well-verified and widely used ORIGEN burnup/depletion tool. The main drawback to this method is time; Monte Carlo methods are very slow by comparison with transport codes, but the main advantage is the simplicity of defining geometry in MCNP [20].

Something must be said about the possible error in the calculations with Monteburns, however. There are two places error can arise in these calculations: from the MCNP part or from the ORIGEN2 part of the process. If the number of particles used to calculate the neutron fluxes in MCNP is too small, or too few iterations are used, the answer will not converge before the calculation is finished. One way of mitigating this without inordinately increasing computer time is to run inactive k_{eff} cycles in MCNP. Fluxes are not tallied in inactive cycles, but are used to improve the initial guess of k_{eff} so that when the fluxes begin to be tallied during the active cycle, the answer is already closer to being converged. These calculations were performed with sufficient particles and inactive cycles to achieve a converged answer with an error less than 1%, as estimated by MCNP.

Another place error can arise is during the ORIGEN2 calculations. If the time steps given to Monteburns are long, the amounts of materials change too quickly, and inaccurate fluxes are calculated after the materials are fed back into MCNP. If the time steps are short enough, the error gets quite small. As Charlton et al. described in their benchmarking study of the Monteburns code, for PWR pins a time step of 2,000 MWd/MT or less gives errors that are effectively zero. A time step of 5,000 MWd/MT agrees with the converged solution within 1%, and even 10,000 MWd/MT corresponds to less than 4% error, maximum [21].

Series I System Description

The system used for the Series I fuel modeling is a typical Westinghouse pressurized water reactor, chosen because of its widespread use and the resulting large

amount of data on it [22]. In these 17x17 assemblies, there are 289 available pin positions, but only 264 are used for fuel while the other 25 positions are either water holes or positions for control rods. The MOX assemblies have only water holes and no control rods in this model. Some of this data is listed in Table 1.

Table 1
Some Westinghouse PWR core specifications

Parameter	Fresh	Once-Burned	Twice-Burned	MOX	Total
Number of Assemblies	44	44	45	60	193
Number of pins per assembly	264	264	264	264	50,952
Number of control assemblies	20	40	12	0	52
Starting Enrichment (fissile Pu in MOX assembly)	4.0%	2.8%	1.4%	5.5%	n/a
Height of Fuel Assemblies (cm)	366	366	366	366	366
Radius of Fuel Pins (cm)	0.475	0.475	0.475	0.475	0.475
Pin Pitch (center to center) (cm)	1.26	1.26	1.26	1.26	1.26

There are several reasons for using a thermal spectrum system for this first stage of spent fuel transmutation, and not having solely a one tier, fast spectrum actinide burner. First of all, there is much worldwide experience in using MOX to fuel thermal reactors (Europe and Japan both do this quite readily, and with good results). Secondly, it is a good way to burn plutonium safely, which is quite reactive and also a concern from a nonproliferation standpoint, without separating it from the uranium. Essentially, it amounts to extending the burnup of current LWR fuels, since in the normal operation

of low-enriched uranium LWR cores, a significant fraction of the power generated by the fuel later in the cycle is generated by the plutonium that is bred in earlier in the cycle.

Third, with the addition of neptunium to the fuel, if a small amount of neptunium is added to the MOX fuel, there is little impact on the fuel with regard to neutronics or safety, and the thermal absorption cross section of ^{237}Np can be advantageous due to the additional production of plutonium which will contribute to extending the burnup. From a long-term standpoint, a Japanese/Russian study by Nikitin et al. on the neptunium content of MOX fuels led to setting the neptunium concentrations between 0%and 4% to both extend burnup and increase the transmutation of this isotope [5]. The plutonium content was set at 7.6% and the rest of the MOX fuel form is depleted uranium. Reactor-grade plutonium was used, consisting of 58% ^{239}Pu, 24% ^{240}Pu, 14% ^{241}Pu, and 4% ^{242}Pu. The fuel choices ranged over the compositions given in Table 2 for the Series I fuels. The densities of all the fuels were taken to be 85% TD, the theoretical densities for MOX and for UO_2 being 11.08 g/cm^{3}and 10.96 g/cm^3, respectively [23,24].

Single Pin Calculations

First, individual pins of this Westinghouse PWR design were modeled in an infinite lattice with the standard fuel and with various MOX compositions for comparison. Table 2 shows the first series of fuels modeled.

The k_{eff} values calculated with MCNP/Monteburns for these single MOX pins, indicating their reactivity, have been plotted against the reference PWR pin with 4.01% enriched UO_2 fuel, and the results are in Fig. 1. As can be seen, the reactivities of all the MOX pins are much higher than that of a standard pin. This would be expected, since

the fraction of fissile material is higher (5.47% ^{239}Pu + ^{241}Pu versus 4.01% ^{235}U). For comparison, MOXpin6 has a fissile fraction equal to that of the reference PWR pin, with a k_{eff} at the beginning of the cycle of 1.24 as compared to 1.13 for the standard pin and 1.32 for the 0% Np MOX pin. This demonstrates that any MOX fuel is always going to be more reactive than standard LEU reactor fuel. This result follows from the much larger thermal fission cross section values for ^{239}Pu and ^{241} Pu with respect to ^{235}U (750 and 1010 barns versus 585 barns, respectively), and it is exaggerated even more in these MOX fuels, with their larger fissile fractions than the reference reactor fuel. This requires careful placement when put into the reactor, which will be discussed later.

Table 2
MOX compositions for the Series I PWR

Run	% Pu	% Np	% Depleted Uranium
PWRpin	0.0%	0.00%	4% ^{235}U enriched
MOXpin1	7.6%	0.00%	92.4%
MOXpin2	7.6%	0.04%	92.0%
MOXpin3	7.6%	2.00%	90.4%
MOXpin4	7.6%	3.00%	89.4%
MOXpin5	7.6%	4.00%	88.4%
MOXpin6	5.6%	0.00%	94.4%

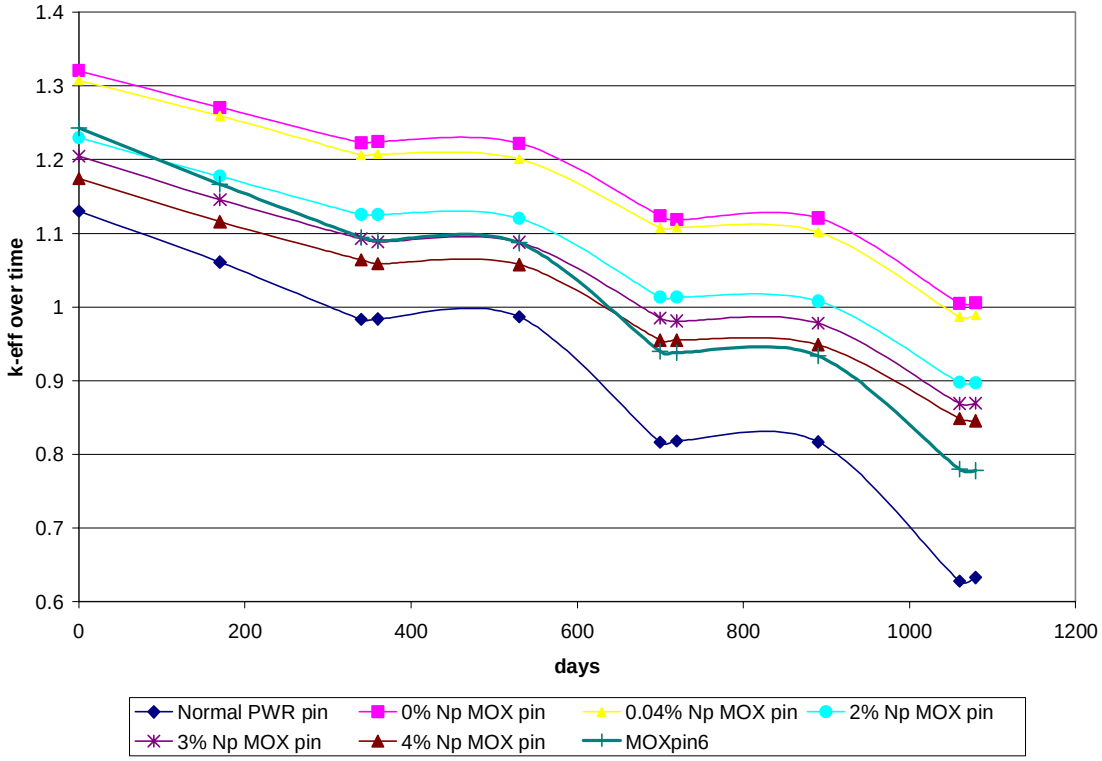

Fig. 1. k_{eff} measurements over 1,080 day cycle with three, 30-day no-power decay periods.

The error associated with these calculations is given in Table 3 below. The calculations were performed using 2 source points per 366 cm long fuel rod. This would seem not very accurate, since the Monteburns output gives us a macroscopic fission cross section (Σ_f) for these fuels of between 3.97 cm^{-1} for the regular PWR pin to 5.26 cm^{-1} for the 0.0%Np MOX pin (the largest value). Of course, the macroscopic cross section is related inversely to the mean free path in the material by:

$$1\,\mathrm{MFP} = \frac{1}{\Sigma_f} \tag{2.1}$$

which gives an average mean free path of between 0.19 cm for the MOX and 0.25 cm for the UO_2 fuel.

Table 3
Error associated with k_{eff} calculations per burn step

Days	PWRpin	MOX 1	MOX 2	MOX 3	MOX 4	MOX 5	MOX 6
0	0.18%	0.29%	0.28%	0.24%	0.26%	0.25%	0.24%
170	0.17%	0.25%	0.26%	0.23%	0.21%	0.20%	0.20%
340	0.16%	0.24%	0.21%	0.24%	0.20%	0.19%	0.23%
360	0.18%	0.26%	0.26%	0.20%	0.21%	0.21%	0.22%
530	0.13%	0.22%	0.22%	0.18%	0.18%	0.18%	0.20%
700	0.13%	0.21%	0.20%	0.20%	0.19%	0.15%	0.17%
720	0.13%	0.22%	0.23%	0.20%	0.17%	0.17%	0.18%
890	0.10%	0.20%	0.19%	0.17%	0.18%	0.14%	0.13%
1060	0.08%	0.18%	0.17%	0.15%	0.16%	0.13%	0.11%
average	0.14%	0.23%	0.23%	0.20%	0.19%	0.18%	0.19%

Despite this, increasing the number of source points would not have much of an effect on the accuracy for the single pin models, due to the way MCNP works. MCNP uses the neutrons generated from the previous generation (as in real life) as the source for the current cycle, and so really only one source point per fissionable region is necessary to get good results.

In addition, the user of MCNP can run inactive k_{eff} calculation cycles, in which MCNP starts particles and keeps track of them but doesn't perform the more time-consuming tallies, which is a good way to increase the accuracy for a smaller investment in computer time. The most important thing is to run enough k_{eff} cycles, and the accuracy reflected in Table 3 would indicate that 200 cycles, with 100 active, is

sufficient. The error bars in Fig. 1 are smaller than the display size of the points on the chart.

The following plot, Fig. 2, shows the net change in each isotope of interest for each fuel composition at the end of the burn cycle. A 1,080 day burn cycle was used, consisting of 3 cycles of 340 full power days followed by a 20 day decay period representing the outage. In the full core model, fuel will be shuffled as in a real reactor.

This chart shows us no real surprises. The amount of ^{238}Pu increases with increasing initial neptunium fraction, due to the following reactions:

$$^{237}Np + n \xrightarrow{150\ \text{barns}} {}^{238}Np + \gamma \tag{2.2a}$$

$$^{238}Np \xrightarrow{2.117\text{d}} {}^{238}Pu + \beta^{-} \tag{2.2b}$$

However, this ^{238}Pu will become ^{239}Pu if it remains in the reactor or is reprocessed and put into another reactor, and can then provide fissile material, due to the huge (n,γ) cross section of ^{238}Pu. Over an extended burnup, this could help stabilize the reactor power as it would be a good source of ^{239}Pu, as well as getting rid of the undesirable neptunium.

It is useful to compare this chart with the same data normalized to the initial amount of each isotope in the fuel at the beginning of the cycle. This is shown in Fig. 3.

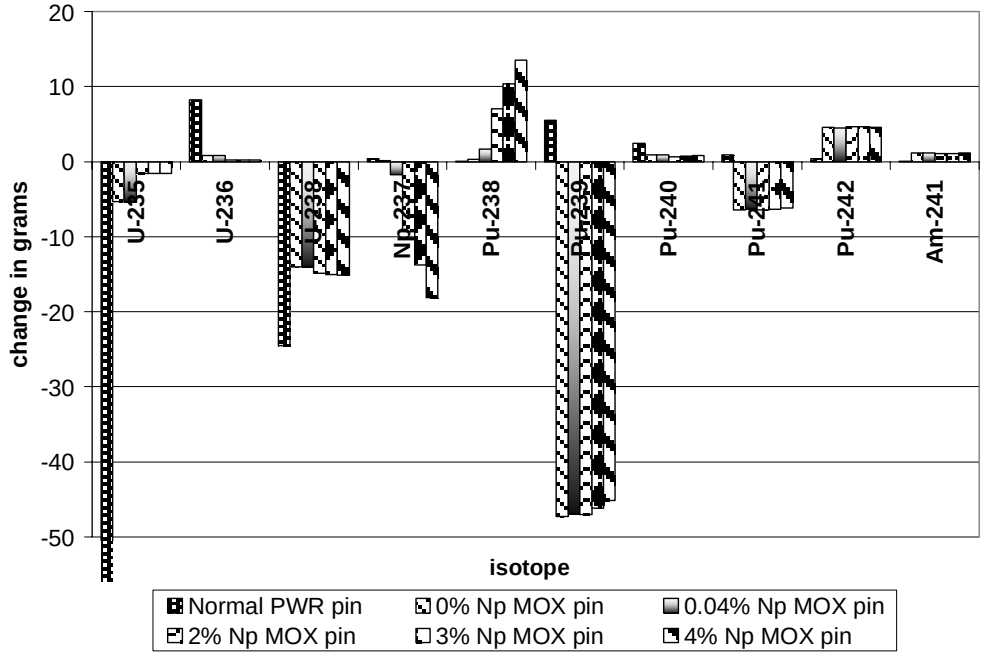

Fig. 2. Net change in the amount of uranium, neptunium, plutonium and ^{241}Am for a single PWR fuel pin at 42,000 MWD/MTHM burnup. Curium not included because amounts are too small to appear on this chart.

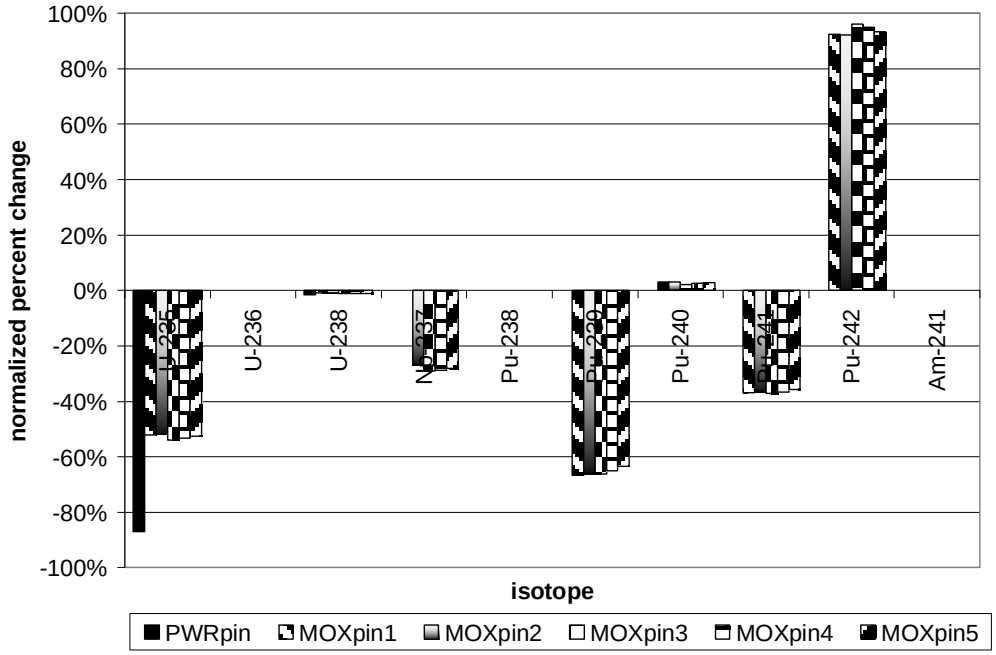

Fig. 3. Normalized percent change in uranium, neptunium and plutonium inventory, PWR pins.

Between the various compositions of MOX, there is little difference in the amount of plutonium consumed – the main advantage of adding neptunium to MOX is that not only does it burn the neptunium, but it decreases the reactivity of the pin, as shown previously in Fig. 1. This makes it more comparable to the reference PWR pin, and therefore easier to place into the reactor. Based on this data, the best transmutation fuel among these pins is the 4% Np MOX rod. Unfortunately, spent fuel contains only about 0.02%-0.07% Np [25]. Unless there is a complicated reprocessing stream, involving the separation of neptunium from vast quantities of spent fuel to provide enough to make MOX rods with 4% Np, one of the lower-Np compositions will have to be chosen for the sake of practicality.

However, the higher Np-containing fuel will also be modeled as it is the best from a transmutation standpoint, and also because when reprocessing is developed and instituted, the first task will be burning all the existing spent fuel inventory. Thus, it would be advantageous to put as much of the neptunium, plutonium and minor actinides into as few transmutation systems as possible. This study does not deal with the details of reprocessing, but it stands to reason that the farther the transmutation fuel composition diverges from the composition of the unprocessed spent fuel, the more potentially difficult, lengthy and expensive the reprocessing procedure will be. This is an issue that cannot be ignored, but for the purposes of this study, only the calculation of the best transmutation fuel will be considered.

Whole Core Calculations

Since the decision has already been made by the Department of Energy that the Series I thermal spectrum system will be along the lines described in the introduction, and because the focus of this work is on the fast reactor system, only a few runs were performed. These represent the best fuels from the single pin analyses performed, and so have been put into the whole core model. The whole core analysis will therefore be using the 0.0% Np MOX, the 0.04% Np MOX, and the 4% Np MOX. Since, as stated before, this fuel has the best transmutation efficiency of neptunium, with comparable performance for plutonium and minor actinides, it would require complicated reprocessing to extract neptunium from spent fuel and put it into a transmutation fuel to give 4 wt%.

Fig. 4 shows a possible core layout of a typical Westinghouse pressurized water reactor, and the chosen layout for the Series I fuels transmutation core [26]. The normal assemblies that have been replaced with MOX are indicated in blue with diagonal stripes. The ¼ core layout was used to simplify the MCNP input file for the Monteburns code, and well approximates a full core by using reflecting boundary conditions on the two sides that have symmetry with the rest of the core. The MOX assemblies in the transmutation core represent slightly less than a $^{1}/_{3}$ core loading of MOX fuel, about 32% by volume.

Fig. 5 shows the location of the control rod assemblies in a standard core – this same layout was used in the transmutation core despite the replacement of some standard

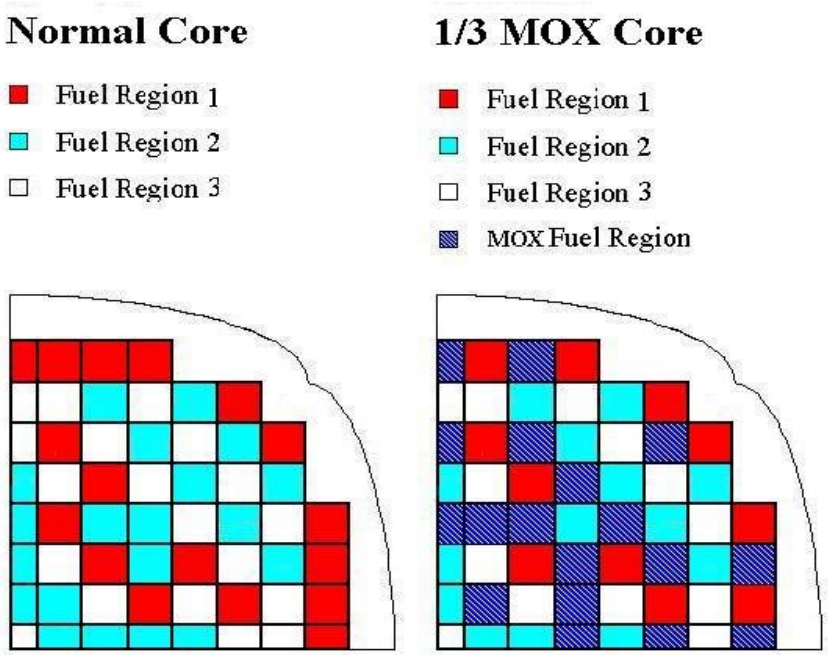

Fig 4. Standard PWR ¼ core model with fresh, once- and twice-burned fuel, and the location of MOX fuel assemblies with respect to original layout, 32% MOX loading.

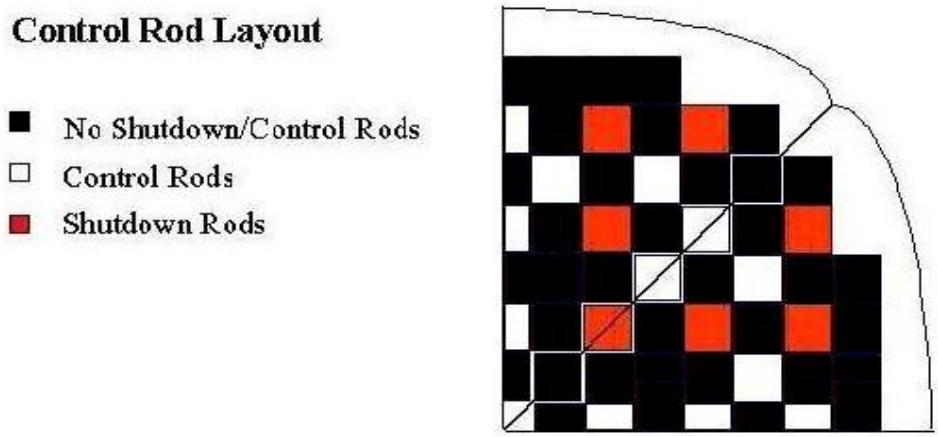

Fig. 5. Control rod locations.

assemblies with MOX assemblies. None of the MOX assemblies have control rods of either kind within them. These figures have been adapted from "Reduction of the Radiotoxicity of Spent Nuclear Fuel Using a Two-Tiered System Comprising Light

Water Reactors and Accelerator-Driven Systems", Holly R. Trellue, doctoral dissertation, University of New Mexico Department of Nuclear Engineering, 2003 [26]. Table 4 contains the description of these core layouts.

Table 4
Some numbers on the PWR and MOX core models

	# of Assemblies	# w/ control rods	Volume, cm^3	% volume
Normal Core				
Fresh Fuel	64	20	3.478E+06	33%
Once-Burned	64	40	3.382E+06	32%
Twice-Burned	65	12	3.573E+06	34%
MOX core				
Fresh Fuel	44	20	2.361E+06	23%
Once-Burned	44	40	2.265 E+06	22%
Twice-Burned	45	12	2.456 E+06	23%
MOX	60	0	3.352 E+06	32%

The calculations of the burnup of materials for the standard core and the three MOX cores are shown below, in Fig. 6, and these amounts normalized to the initial feed per isotope are displayed in Fig. 7. The control rods have not been moved, simply modeled as fully in. In addition, no modeling was done of the boron concentration in the coolant. 500 ppm ^{10}B was included in the water in the model at the beginning, and this was not varied over the course of the burn cycle. The cores have been modeled for one burn cycle of 360 days duration. Thus, in one year's time, for the 4% Np MOX core, over 500 kg of plutonium and 150 kg of neptunium can be burned. The buildup of ^{242}Pu is large in the MOX cores, but will likely become ^{243}Am and then be burned in the fast reactor system. The buildup of ^{240}Pu is comparable to that for the standard PWR core, and the 120 kg of ^{238}Pu is directly a result of the neptunium (n,γ) reactions. The most

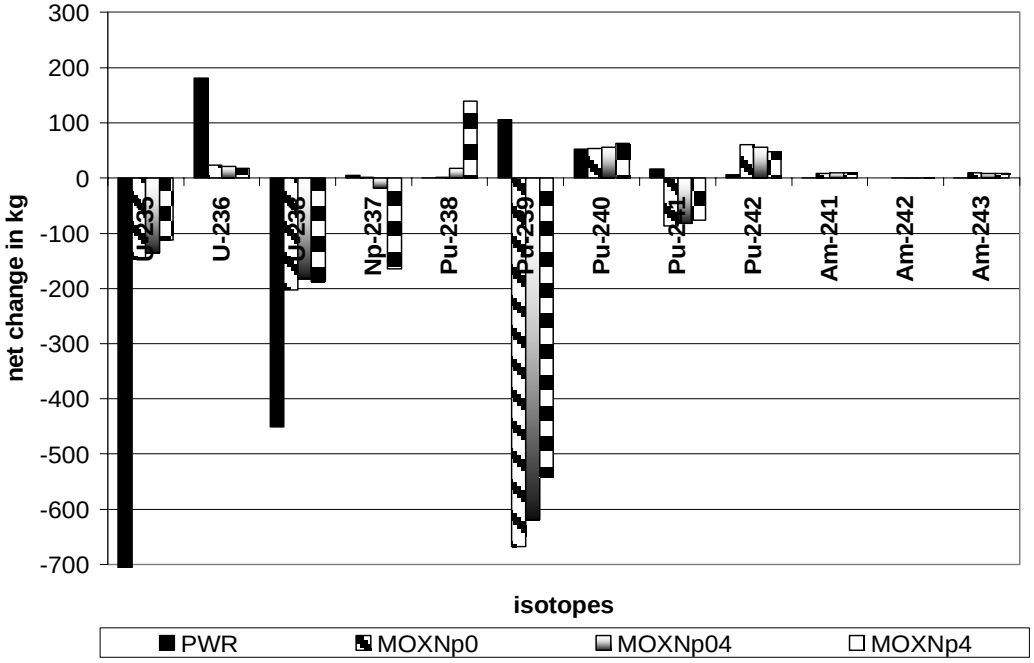

Fig. 6. Net change of U, Pu and Am for PWR and 1/3 MOX fueled whole cores, 360 day burn.

interesting part of this plot is the amount of ^{235}U burned – a significant amount more in the 4% Np MOX core than in either of the other two MOX cores. The initial feed is about 100 kg less in the 4% Np MOX core, and yet the net decrease in the amount of ^{235}U is over 100 kg more than in the cores that start with a higher uranium fraction. By increasing the fraction of neptunium and decreasing the amount of uranium, we have encouraged the core to burn more fissile uranium than plutonium. This could be an effect of the different neutron spectrum in the core as a result of the added neptunium. The fraction of plutonium in all of these MOX pins is 7.6 wt.%, and the only difference is the amount of neptunium (and thus, depleted uranium, which makes up the bulk in these MOX fuels).

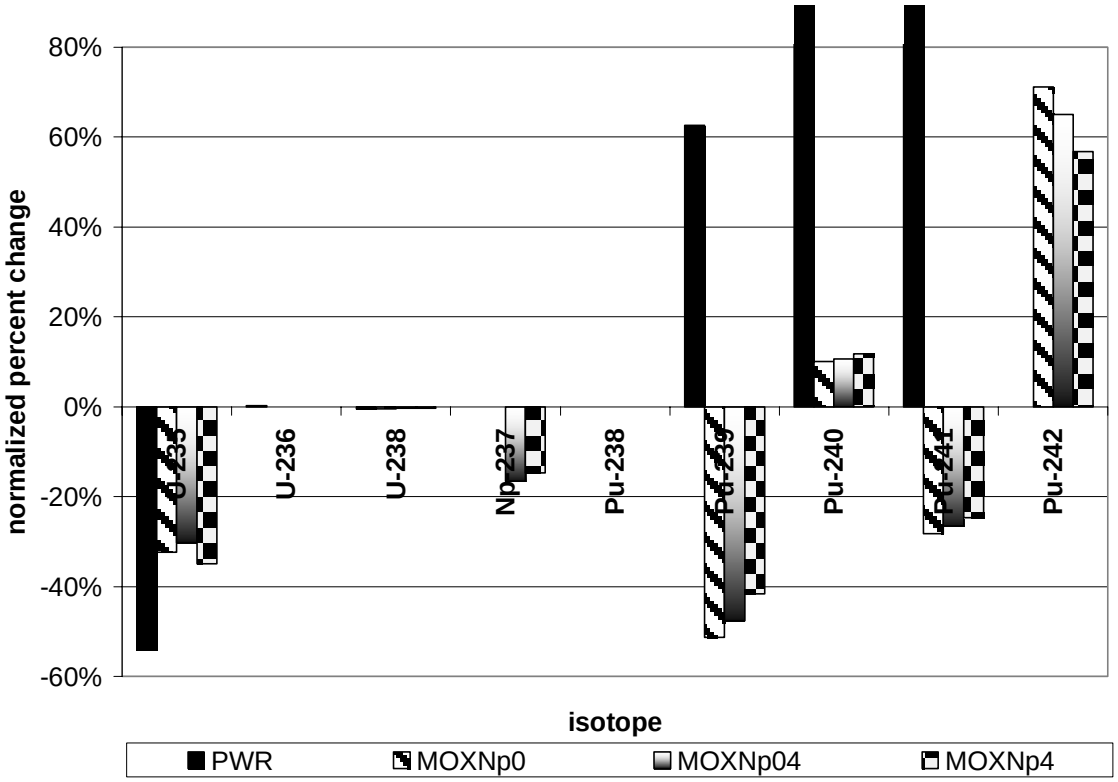

Fig. 7. Normalized percent change of U and Pu isotopes for normal and 1/3 MOX fueled PWR cores.

From a percentage standpoint, the 0.04% MOX fuel gives the best results overall, because it burns plutonium at a rate in between the other two fuels, an average of 20.5%, taking into account all the isotopes. In addition, the plutonium is significantly degraded from a reactor fuel standpoint and also from a weapons standpoint, which increases its proliferation resistance somewhat, due to the buildup of non-fissile isotopes ^{240}Pu and ^{242}Pu. In addition, the 0.04% MOX fuel seems to do the best because although it burns far less neptunium per 360 day cycle, it burns a slightly better percentage of the initial feed neptunium, 15.5% compared to 14.7% of the neptunium in the 4% Np MOX core. However, if it is more desirable to burn a great deal of neptunium at the expense of some

plutonium transmutation efficiency, the 4% Np MOX core burned almost 150 kg of neptunium in one year. This is a priority that will be addressed to some extent in chapter IV, in which we will discuss which isotopes are most vital to eliminate in spent fuel from a repository standpoint.

Delayed Neutron Information

The delayed neutron fraction is the fraction of the total neutrons emitted during fission that are not emitted immediately, but after a short delay time. The presence of delayed neutrons from the fission of uranium is the main reason that reactors can be controlled, because in a critical reactor, the chain reaction is always dependent on the previous generation of fissions as well as the current generation. This provides a time delay between the prompt neutron emissions and the delayed neutrons, equal to the time of decay of the fission fragments ($\lambda \approx 0.08\ s^{-1}$). The delayed neutron fraction for a typical ^{235}U fueled reactor is around $\beta \approx 0.0075$ [25].

The delayed neutron fraction for any fuel can be calculated by the following method, using the data in tables A.1 and A.2, found in Appendix A:

$$\beta_i^j = \frac{1}{100}\frac{\alpha_i^j \nu_d^j}{\nu^j}, \tag{2.3}$$

where

β_i^j = delayed neutron fraction for group i and isotope j
ν_d^j = the number of delayed neutrons emitted per 100 fissions for isotope j
ν^j = total neutron yield for isotope j
α_i^j = the delayed neutron 6-group parameters for isotope j, i = 1,2..6.

The ν_d^j values were taken from table A.1, and the α_i^j's from table A.2 in Appendix A. Then, the averages of the β_i^j's for isotope j, weighted by the microscopic fission cross section σ_f^j and the number density (in nuclei/cm^3) N^j (i.e., by the macroscopic fission cross section), are taken:

$$\overline{\beta_i} = \frac{\sum_j \sigma_f^j N^j \beta_i^j}{\sum_j \sigma_f^j N^j} \tag{2.4}$$

which gives the average delayed neutron fraction for time group i, i = 1,2…6. These are then simply summed over the time groups to give the total delayed neutron fraction:

$$\overline{\beta} = \sum_j \overline{\beta_i} \tag{2.5}$$

The delayed neutron results for the fuels that were used in the individual pin models are displayed below in Table 5. The average delayed neutron fraction for the MOX pins, which didn't vary much with respect to the neptunium content, was around 0.0034, or only about half of that for a uranium pin. Calculations for a normal PWR pin at the end of the cycle gave $\beta \approx 0.0076$. The beginning-of-cycle data gave $\beta \approx 0.0082$, which makes a cycle average value of 0.0079. This has an error of ± ~5% with regard to the Stacey value of 0.0075 [25]. Thus, this method can be used with confidence to give a fair estimate of the delayed neutron fraction in these fuels. As can be seen, adding neptunium to the MOX pin doesn't change the delayed neutron fraction very much. The delayed neutron fraction for a normal MOX pin (pins 1 and 6 in this table, essentially) is

only about half of that of a normal PWR pin, but since MOX has a long history of use, adding neptunium to the mixture yields little change.

Table 5
Delayed neutron fractions for different Series I MOX fuels, end of cycle

Run	% ^{235}U	% Pu	% Np	β
PWR pin	2.31%	0.3%	0.01%	0.007587
MOXpin1	0.48%	7.6%	0.00%	0.003597
MOXpin2	0.48%	7.6%	0.04%	0.003559
MOXpin3	0.14%	7.6%	2.0%	0.003377
MOXpin4	0.14%	7.6%	3.0%	0.003398
MOXpin5	0.14%	7.6%	4.0%	0.003386
MOXpin6	0.18%	5.6%	0.0%	0.003440

The delayed neutron fractions for the whole-core models are below in Table 6. These were computed by taking averages over all the materials in the whole core. Monteburns calculates material-averaged cross section sets and whole-model ν values, which can then be used to calculate a rough estimate of the whole core delayed neutron fraction.

Table 6
Delayed neutron fractions for whole core PWR model and 1/3 MOX fueled PWR cores, end of 360 day cycle

Run	% ^{235}U	% Pu	% Np	β
PWR	1.19%	0.46%	0.01%	0.006884
MOXNp0	1.41%	1.98%	0.00%	0.005378
MOXNp04	1.38%	2.46%	0.11%	0.004896
MOXNp4	1.12%	2.32%	1.11%	0.004974

Due to the fact that the PWR core modeled here does not contain entirely fresh UO_2 fuel but rather a cycle-average composition in which there are three zones of fuel, which represents a PWR with roughly a 12 month fuel cycle and a 1/3 core replacement loading each time, there is a some plutonium in the core and thus the delayed neutron fraction is lower than that calculated for fresh UO_2 pins in the previous section.

Chapter Summary

In this chapter PWR pins and whole cores were modeled with various compositions of neutron-containing MOX fuels. Results showed that adding neptunium to normal MOX produces little change, and the change is in fact positive in that it reduces the reactivity to a more manageable level. This, in turn, makes it easier to place these fuels into the reactor. The effect of MOX fuels and neptunium-containing MOX fuels on the delayed neutron fraction was also examined, and found that it is workable to fuel a reactor with a 1/3 core MOX loading.

In addition, using these fuels also helps to accomplish the task for which Np-MOX is being considered in the first place: burning neptunium along with plutonium in a thermal spectrum reactor to reduce the amount of these isotopes in spent fuel, and thus the load on a repository. Interestingly, a smaller amount of neptunium was found to burn a larger fraction of that neptunium, and also left more neutrons available to transmute the plutonium. The impact of this on the fast spectrum system will be seen in Chapter IV, through the evaluation of a closed fuel cycle for thermal production reactors, the Series I thermal spectrum transmuter reactors for eliminating neptunium and plutonium, and the fast spectrum Series II systems discussed in Chapter III.

CHAPTER III

SERIES II FUEL CALCULATIONS AND RESULTS

Introduction

The first priority in this study is to determine the best fuel from a transmutation standpoint, that is, the fuel type that transmutes the most plutonium and/or minor actinides per unit time over the cycle length. Thus, there is a need for a fast-spectrum system to effectively do this. There are other issues, however, that need to be addressed beforehand. First of all, the reactivities of the transmutation fuel pins need to be compared to the standard pins for the fast spectrum system, to see if they will be possible fuel choices from a criticality standpoint. In addition, the delayed neutron fractions need to be computed for their effect on reactor safety. The temperature of the fuel is another calculation that affects transmutation efficiency. Since the thermal conductivity of nitride fuels is higher than for the normal MONJU MOX pins, it might be possible to increase the power of the reactor without increasing the fuel centerline temperature over that of the normal MOX fuel and thus go to higher burnup in less time without damaging the fuel. This could be the key advantage of using nitride fuels over oxides in the fast reactor transmutation system. Finally, the main point of this study is to determine how much of the minor actinides can be burned in this system over a given time.

MONJU Description

First, however, an introduction to the MONJU reactor is necessary. The MONJU fast reactor is located near the town of Tsuruga in Fukui Prefecture, Japan. MONJU is a

sodium-cooled fast reactor operated by the Japanese Nuclear Commission. It is not currently in operation, due to circumstances surrounding a minor sodium leak in 1995. However, it is a very interesting and important fast reactor design featuring a high power density and a compact core. It is currently being redesigned to improve safety. Operations are to restart in the future. MONJU is a 714 MWth system fueled primarily with MOX fuel of two different plutonium concentrations, and a depleted uranium blanket of enrichment 0.2% ^{235}U. Some of the design information can be found below in Table 7 [23,24]. Fig. 8(a) and (b) below show different views of the core, to illustrate the relative size of the blanket fuel regions to the inner and outer core regions. Control rod assemblies will not be added to this model because core management and control are not the focus of this study and do not affect the addition of transmutation fuel to the core.

Table 7
MONJU core specifications

	Inner Core	Outer Core	Blanket Region(s)
Number of Assemblies	108	90	172
Number of pins per assembly	169	169	61
Enrichment (Fissile Pu (^{239}Pu + ^{241}Pu)) in inner and outer core and ^{235}U in blanket	14.4%	19.9%	0.2%
Theoretical Fuel Density, g/cm^3	11.06	11.06	10.96
% theoretical density of fuel	85%	85%	93%
Height of Fuel Assemblies	93 cm	93 cm	93 cm outer, 30 cm above, 35 cm below the core
Radius of Fuel Pins	0.27 cm	0.27 cm	0.52 cm
Pin Pitch (center to center)	0.787 cm	0.787 cm	1.315 cm

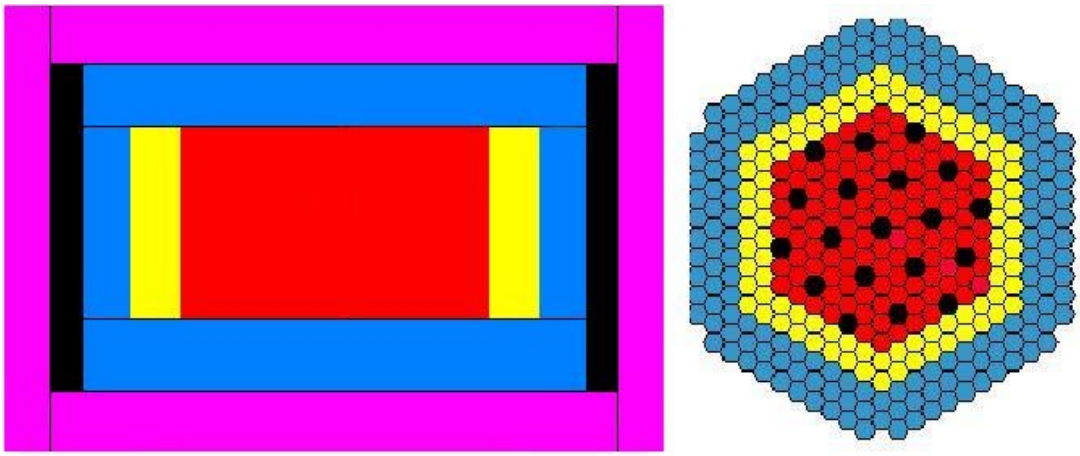

Fig. 8. MCNP plot of MONJU core, vertical view, left, showing the core regions and the axial and radial blankets, and the steel reflector in black. The outermost layer represents the coolant. Horizontal view of inner, outer core and axial blanket, right. The black hexagons represent assemblies containing control rods.

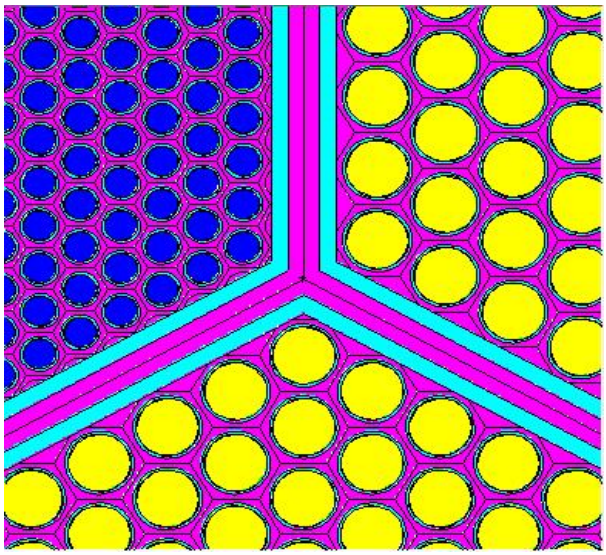

Fig. 9. MCNP plot of the boundary between the core and blanket regions, demonstrating the difference in size of the core and blanket pins.

Fig. 9 shows a close-up of the border between the outer core and blanket fuel regions, to illustrate the difference in size of the core fuel pins versus the blanket pins. More complete design information may be found in Appendix B.

Single Pin Calculations

The main purpose of this study is to determine the effects of using thorium instead of uranium as the base for a transmutation fuel, and, secondly, the effects of using nitride fuel instead of oxide fuel for transmutation. A great deal of potential fuels were modeled and examined comprised of various amounts of plutonium and minor actinide nitrides. The remainder of the fuel is thorium nitride in all cases, except for the fertile free compositions. The neptunium concentration of all pins is 4%. The errors calculated for these pins, using the same method outlined in Charlton et al. for PWR pins, were within the same limits as those in the previous chapter [21]. There was virtually no error calculated as compared with the converged solution for the uranium, neptunium, plutonium, and americium isotopes and very small errors of 2-3% calculated for the curium isotopes with a nearly 10,000 MWd/MT time step.

Thorium Nitride Transmutation Fuels

Two different mixtures of minor actinides were used in these compositions, and are listed in Table 8. The first is an arbitrary mixture, and the second mixture follows the composition of spent fuel given in Stacey's *Nuclear Reactor Physics* [25].

The more interesting and illustrative fuel forms are listed in Table 9 below. These fuels were modeled using the same power level as the normal MONJU core, equal to a power density of 121 W/g, for a whole core total of 714 MWth. Later, the effects of increasing the power will be discussed. The fuel compositions vary between 30 to 90% minor actinide fraction and either 7.6, 6.0 or 4.5% plutonium. The minor actinide fraction is one of the two mixtures of minor actinides from Table 8.

Table 8
Minor actinide mixtures

	Mixture 1	Mixture 2
Am-241	80.00%	26.64%
Am-242	5.00%	0.00%
Am-243	15.00%	73.36%
Cm-242	5.00%	28.94%
Cm-243	5.00%	0.00%
Cm-244	90.00%	71.06%
Cm-245	0.00%	0.00%
Cm-246	0.00%	0.00%
Cm-247	0.00%	0.00%
Cm-248	0.00%	0.00%
Am	80.00%	71.17%
Cm	20.00%	28.83%
	100.00%	100.00%

Table 9
Normal-power MONJU transmutation fuel pins

Actinide Mix 1			Actinide Mix 2		
Run	MA	Pu	Run	MA	Pu
1Mpin41	30%	7.6%	2Mpin41	30%	7.6%
1Mpin42	30%	6.0%	2Mpin42	30%	6.0%
1Mpin43	30%	4.5%	2Mpin43	30%	4.5%
1Mpin44	40%	7.6%	2Mpin44	40%	7.6%
1Mpin45	40%	6.0%	2Mpin45	40%	6.0%
1Mpin46	40%	4.5%	2Mpin46	40%	4.5%
1Mpin47	50%	7.6%	2Mpin47	50%	7.6%
1Mpin48	50%	6.0%	2Mpin48	50%	6.0%
1Mpin49	50%	4.5%	2Mpin49	50%	4.5%
1Mpin51	60%	7.6%	2Mpin51	60%	7.6%
1Mpin52	60%	6.0%	2Mpin52	60%	6.0%
1Mpin53	60%	4.5%	2Mpin53	60%	4.5%
1Mpin54	70%	7.6%	2Mpin54	70%	7.6%
1Mpin55	70%	6.0%	2Mpin55	70%	6.0%
1Mpin56	70%	4.5%	2Mpin56	70%	4.5%
1Mpin57	80%	7.6%	2Mpin57	80%	7.6%
1Mpin58	80%	6.0%	2Mpin58	80%	6.0%
1Mpin59	80%	4.5%	2Mpin59	80%	4.5%
1Mpin61	90%	7.6%	2Mpin61	90%	7.6%
1Mpin62	90%	6.0%	2Mpin62	90%	6.0%
1Mpin63	90%	4.5%	2Mpin63	90%	4.5%

The k_{eff} values for the most reactive fuel pin of each minor actinide concentration are plotted in the next figures. In each case, the most reactive pin was, not surprisingly, the one with the largest plutonium fraction (7.6% Pu). Fig. 10 shows actinide mixture 1 pins with minor actinide concentrations between 30 and 50%, and Fig. 11 shows actinide mixture 1 pins with MA concentrations from 60 to 90%. This is not just to reduce the number of lines per graph, but rather because when the MA concentration goes above 50%, the reactivity of the fuel pin goes above that of the reference MONJU outer core pin. As can be seen in Fig. 11, all of these fuels with 50% or less minor actinides have reactivities in the normal range for MONJU inner and outer core pins.

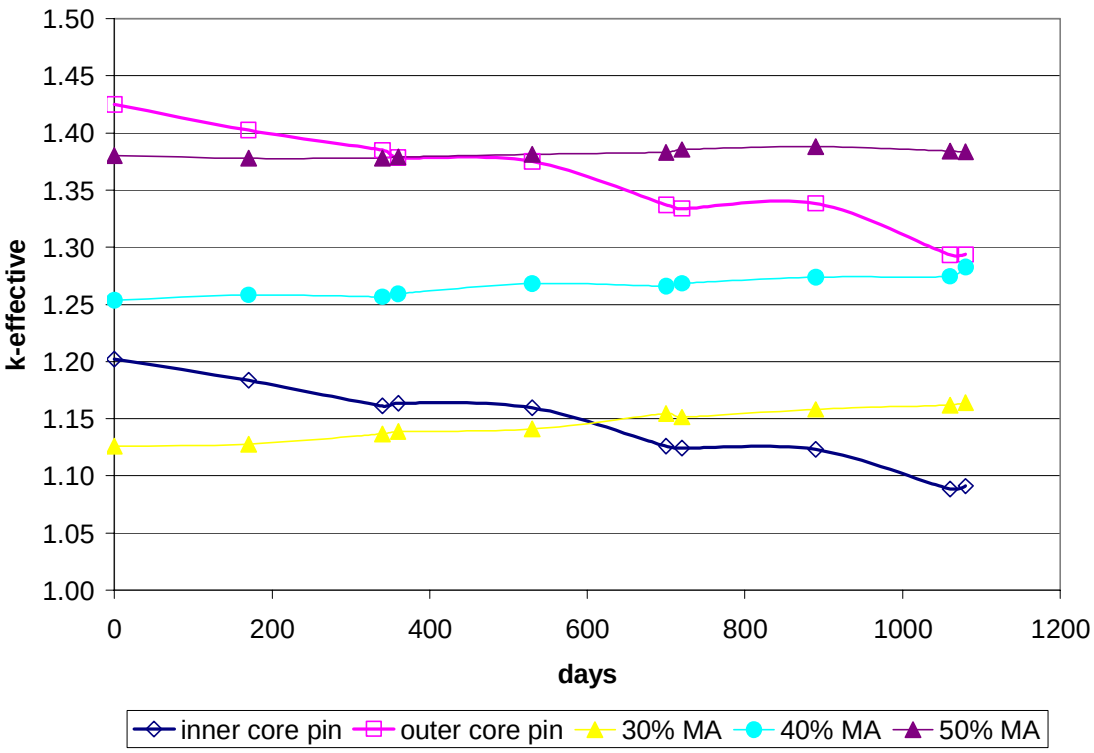

Fig. 10. K_{eff} values of MONJU pins with 30 to 50% minor actinides, MA mix 1.

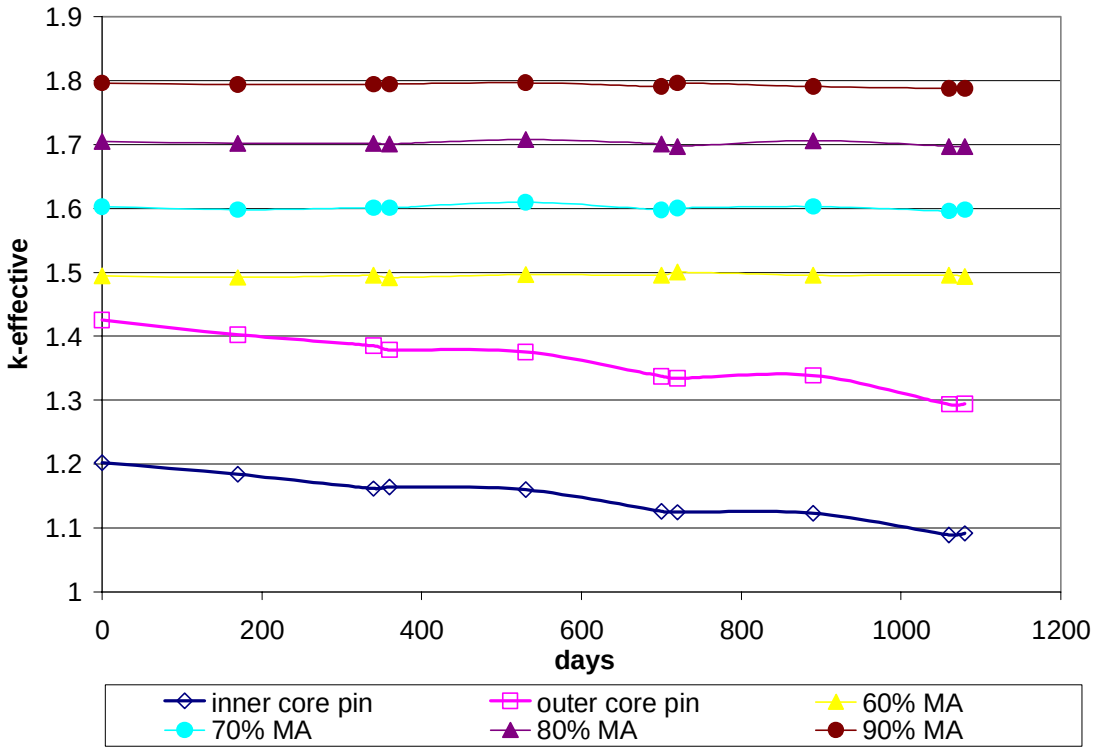

Fig. 11. K_{eff} values of MONJU pins with 60 to 90% minor actinides, MA mix 1.

The objective is the transmutation defined as the amount of plutonium, neptunium, americium and curium transmuted over a given time. In these examples, the pins have been modeled for 3 cycles in the reactor with a duration of 1 year each (340 full-power days plus 20 days of zero-power decay, to represent outage time and fuel handling) for a total of 1,080 days of burn. The net change of all the isotopes in fuels containing 30% MA mixture 1 may be found in Fig. 12.

This chart is interesting for a number of reasons. First of all, in the initial fuels before burning, from left to right the amount of plutonium in the fuel decreases, the balance being made up with thorium. However, the biggest transmutation of thorium and subsequent production of ^{233}U occurred in the middle fuel composition.

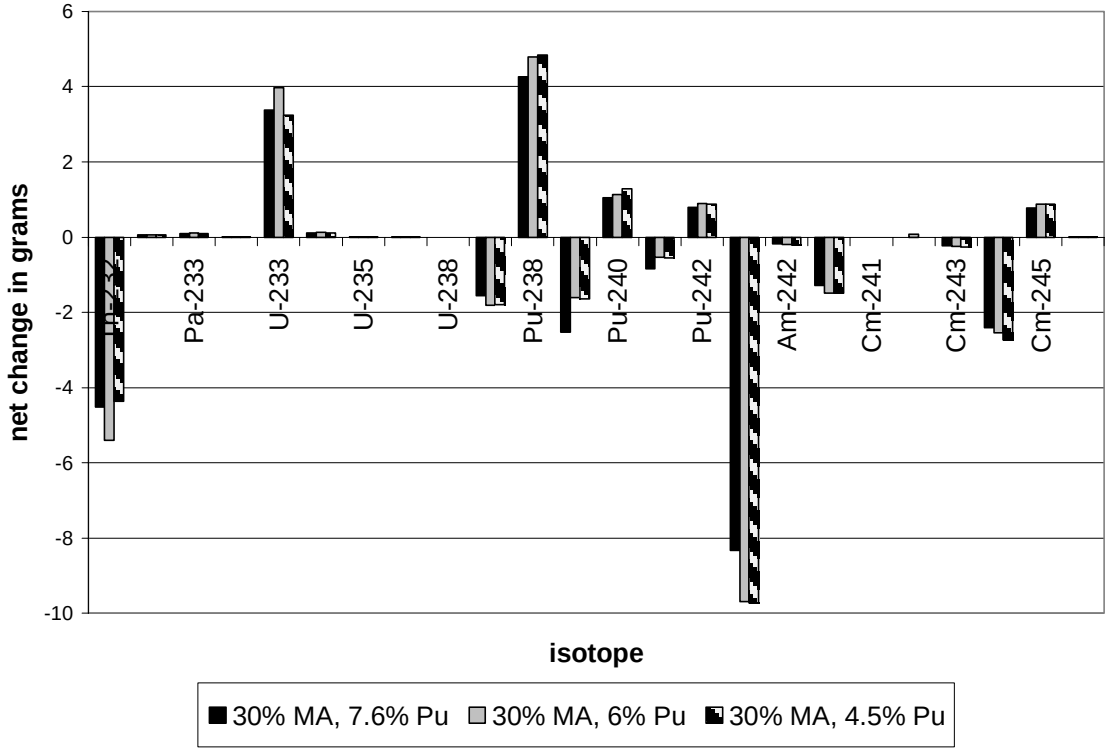

Fig. 12. MONJU pins containing 30% minor actinides, MA mix 1.

Secondly, most of the fission seems to be taking place in the ^{241}Am and not nearly as much in the ^{239}Pu. These have not been normalized, however, so the fact that there is ~20% ^{241}Am in this fuel and only ~4% ^{239}Pu is important. In addition, the ^{238}Pu that was produced probably came from the 6% Cm in the fuel:

$$^{242}Cm \xrightarrow{162.8d} {}^{238}Pu + \alpha \tag{3.1}$$

and the ^{245}Cm was likely produced through this route:

$$\begin{aligned} &^{241}Am + n \rightarrow {}^{242m}Am \xrightarrow{16h} {}^{242}Am + \gamma + n \xrightarrow{1700\text{ barns}} {}^{243}Am + \gamma \\ &^{243}Am + n \xrightarrow{78\text{ barns}} {}^{244}Am + \gamma \xrightarrow{26m} {}^{244}Cm + \beta^- + n \xrightarrow{15\text{ barns}} {}^{245}Cm + \gamma \end{aligned} \tag{3.2}$$

These results, when normalized to the initial amount of each isotope before burning, display a somewhat different picture. This is given in Fig. 13. The zeroes are

not really zero. They are isotopes that were not present in the initial fuel and so they cannot be normalized to an initial amount. The increase of ^{242}Pu 100-200% looks significant. However, less than a gram was produced according to Fig. 12.

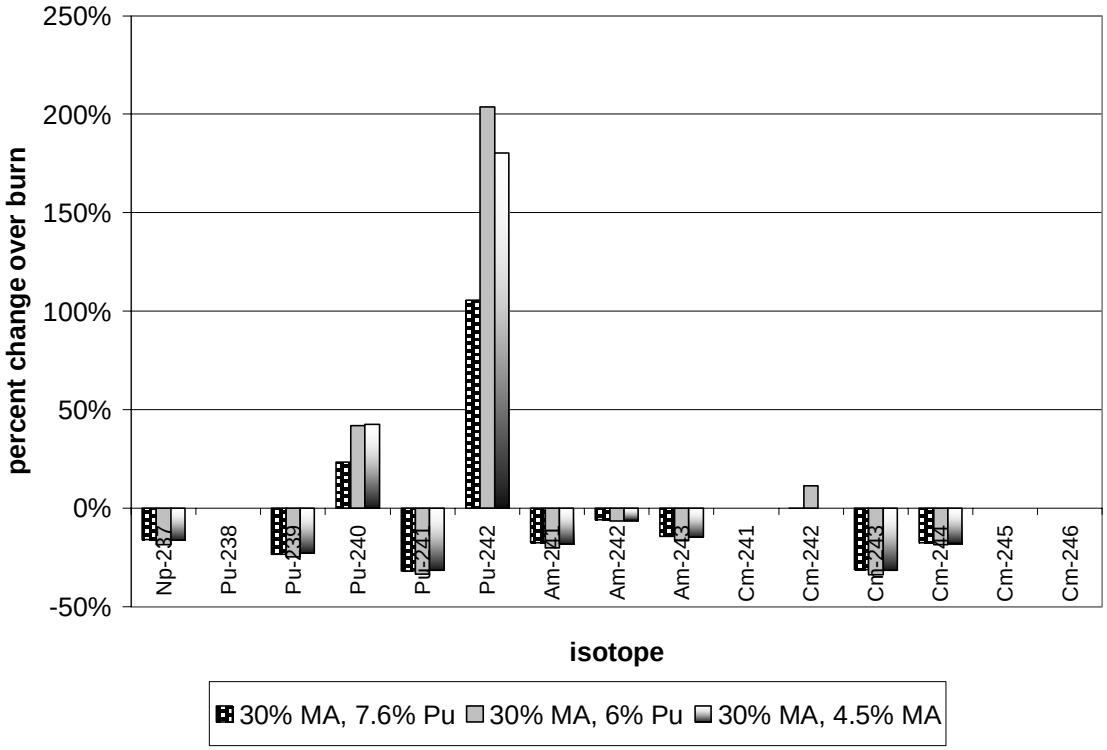

Fig. 13. Normalized percentage changes over burnup for Np, Pu, Am and Cm. 30% MA fuel, minor actinide mix 1.

At the same time, the transmutation of americium which looked so impressive in Fig. 12 looks very unremarkable here on this scale. However, it amounts to -18%, -6% and -15% for the three isotopes, respectively. The transmutation of curium is good as well, except that ^{245}Cm is produced (not shown in Fig. 13).

These were the results for the 30% MA composition using actinide mix 1 from Table 8. The effect of using the different mix of minor actinides needs to be investigated, as well as the effect of increasing the minor actinide concentration from 30% all the way to 90%.

Fig. 14 shows the net change in grams of the same isotopes as Fig. 12, also for 30% MA concentration, but this time showing both actinide mix 1 as before, as well as actinide mix 2, which more closely resembles the output of LWR reactors.

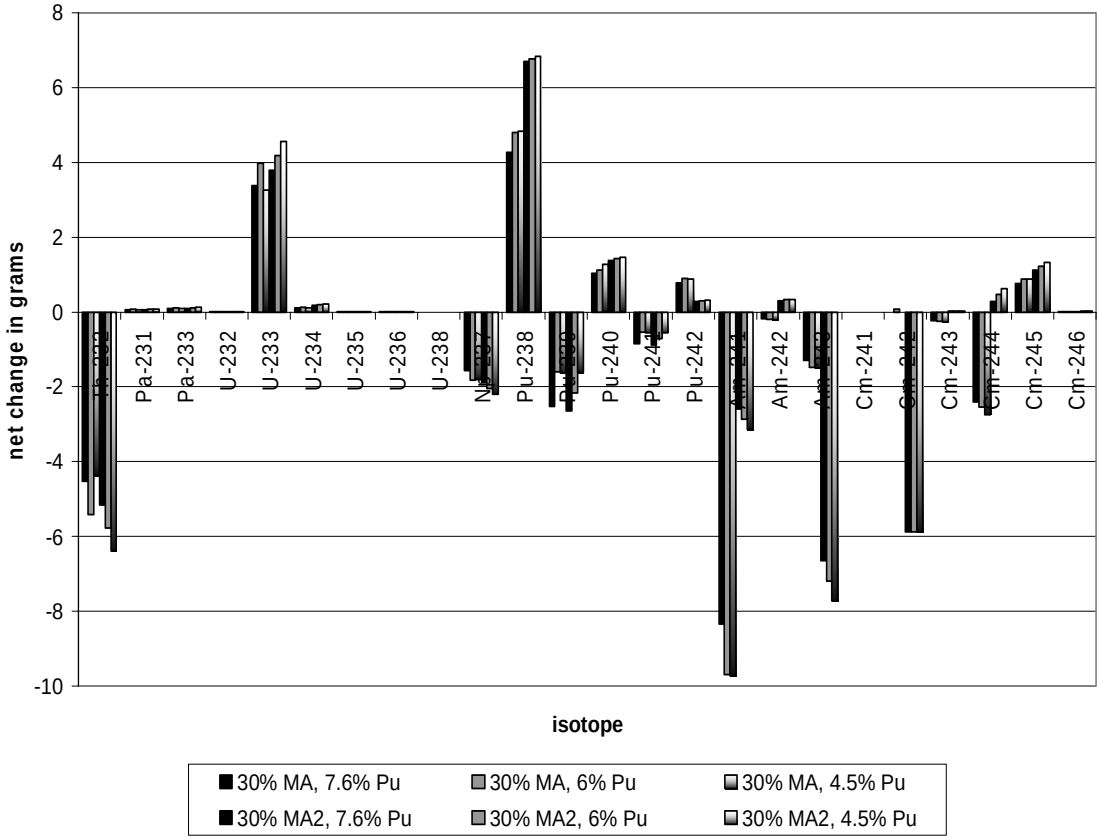

Fig. 14. Comparison of minor actinide compositions 1 and 2, 30% total MA.

This is again not that valuable without looking at the initial concentrations, and thus the normalized results are given below in Fig. 15 for the two different kinds of fuel. The two fuels are quite different in their initial and final compositions.

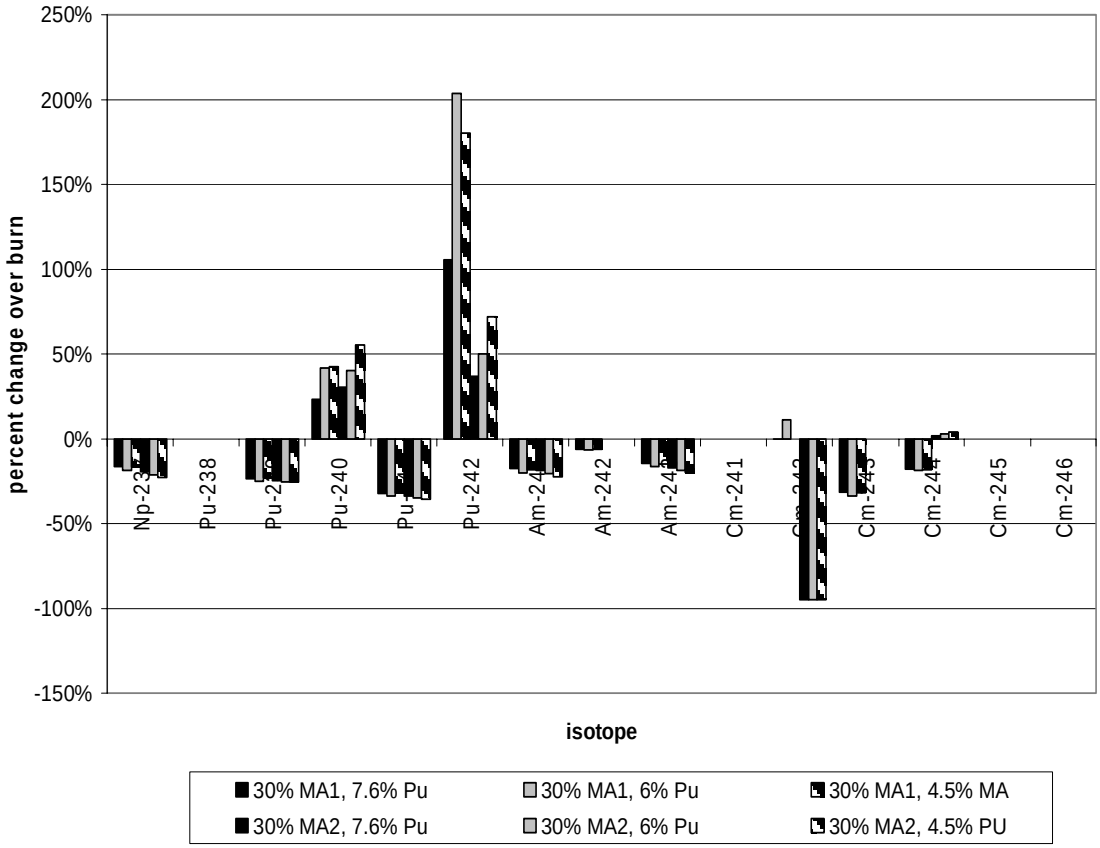

Fig. 15. Normalized comparison of 30% MA fuels, both MA mixtures.

Since the results are more favorable for the second mixture of minor actinides, and also since that composition is a more realistic mixture based on the output of normal light water reactors, it will be the only minor actinide mixture considered for the rest of this study. The arbitrary mixture 1, which did not perform as well as expected, will be

dropped from consideration. The reactivities of these second MA concentration pins need to be plotted, and can be seen in Fig. 16 and Fig. 17. The same division exists as before, in which 50% MA has roughly the same k_{eff} value as the outer MONJU pin. However, the reactivities of these pins increase quite a bit over burnup, although they appear to level off around 2 years in (~700 days burn). This will be important when it is time to put the fuels into the reactor because this increase in reactivity over burn will need to be compensated for somehow.

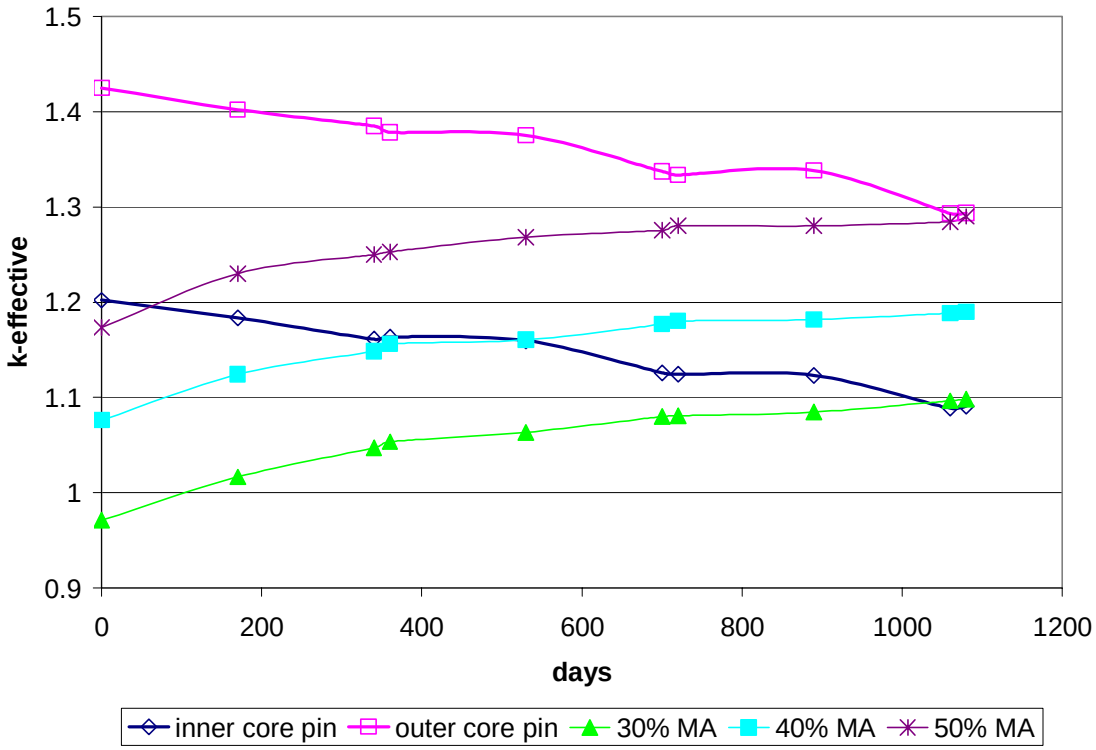

Fig. 16. k_{eff} values for 30-50% MA MONJU pins, minor actinide mix 2.

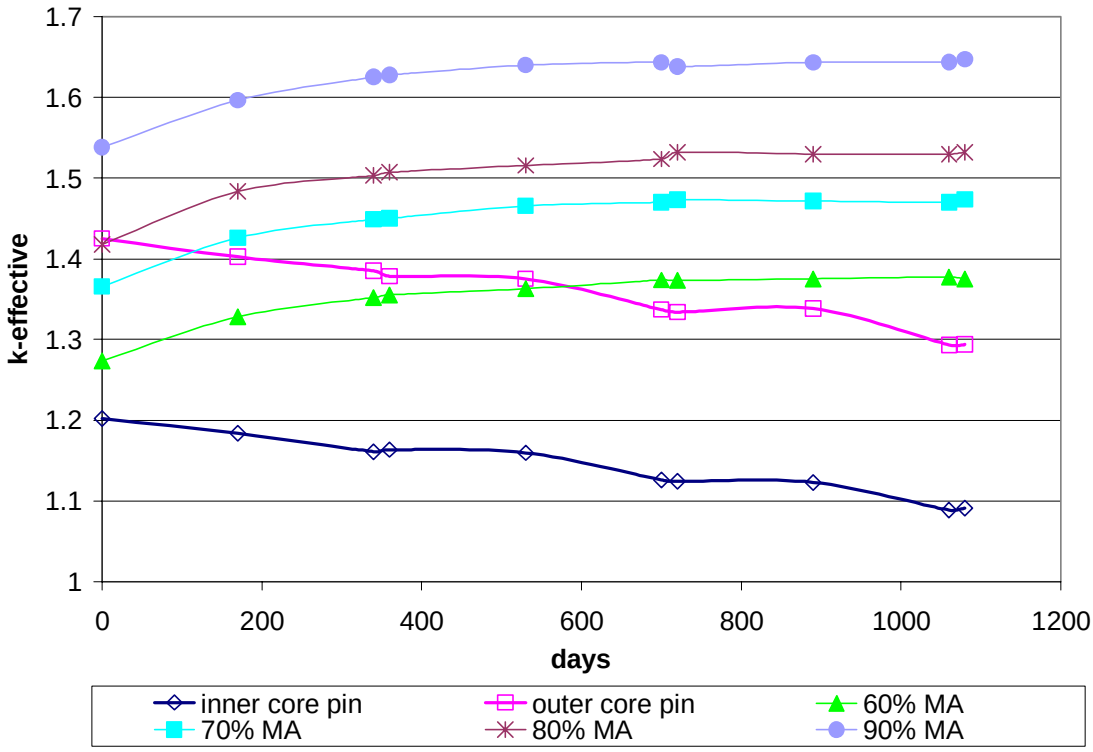

Fig. 17. k_{eff} values for 60-90% MA MONJU pins, minor actinide mix 2.

The one issue with the second minor actinide mix is the even larger fraction of ^{238}Pu which is produced. The heat produced by this isotope is a problem from a handling and storage standpoint. The large ^{238}Pu fraction could potentially be taken care of in the thermal transmutation system, since ^{238}Pu has a 540 barn (n,γ) cross section.

If the plutonium from the MONJU transmutation cycle could be put into a thermal reactor system where it would absorb neutrons and become ^{239}Pu, this would be fissile material to manufacture more MOX fuel with. MOX is needed in a standard MONJU core which gets most of its fissile fraction from reactor grade plutonium. As will be seen later in Chapter IV, the use of MONJU as a transmuter requires more ^{239}Pu than is available as output from the commercial fuel cycle. Therefore, a source of fissile

plutonium is needed in certain core layouts. It is an issue that needs to be addressed and will be discussed in Chapter IV.

Now, the effects of increasing the minor actinide fraction of the fuel need to be investigated. Only the 7.6% Pu fuel will be plotted, because the difference between the results for the 3 different concentrations of Pu in Fig. 6 is not very large, and the k_{eff} values for the 7.6% Pu fuel fall into the normal range for MONJU pins. The results are not very striking in the first plot (Fig. 18), because there are no real deviations from what would be expected. As the minor actinide fraction is increased, the burnup of the minor actinides is increased and the production of ^{238}Pu is increased.

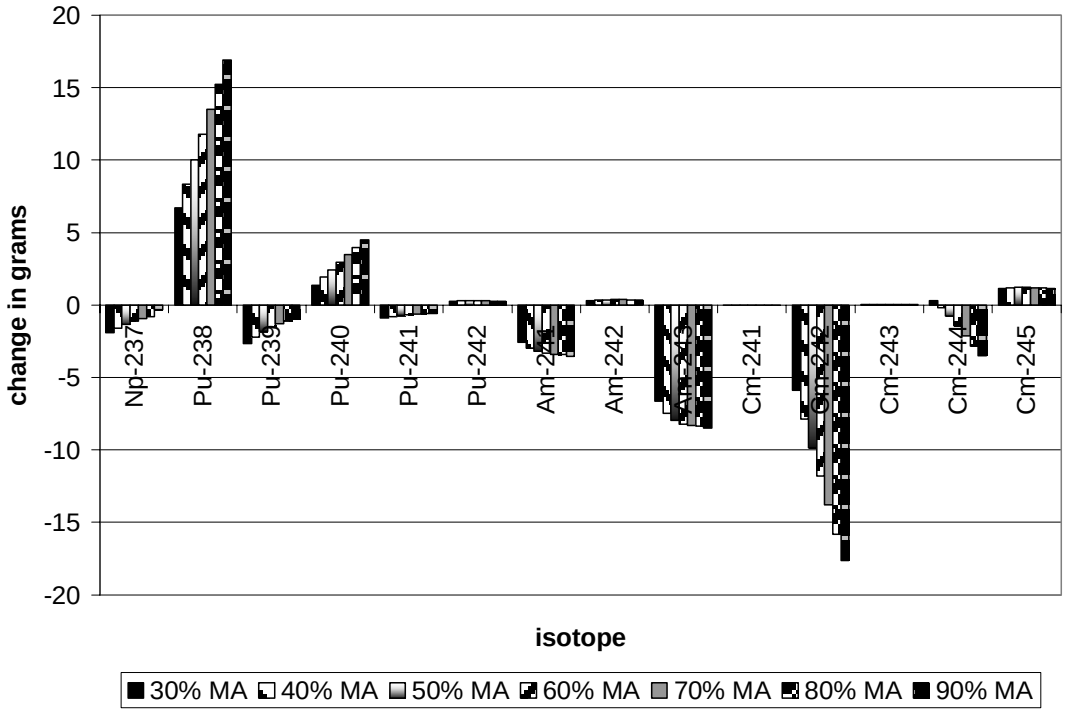

Fig. 18. Change in grams for a 1,080 day burn cycle, 7.6%Pu.

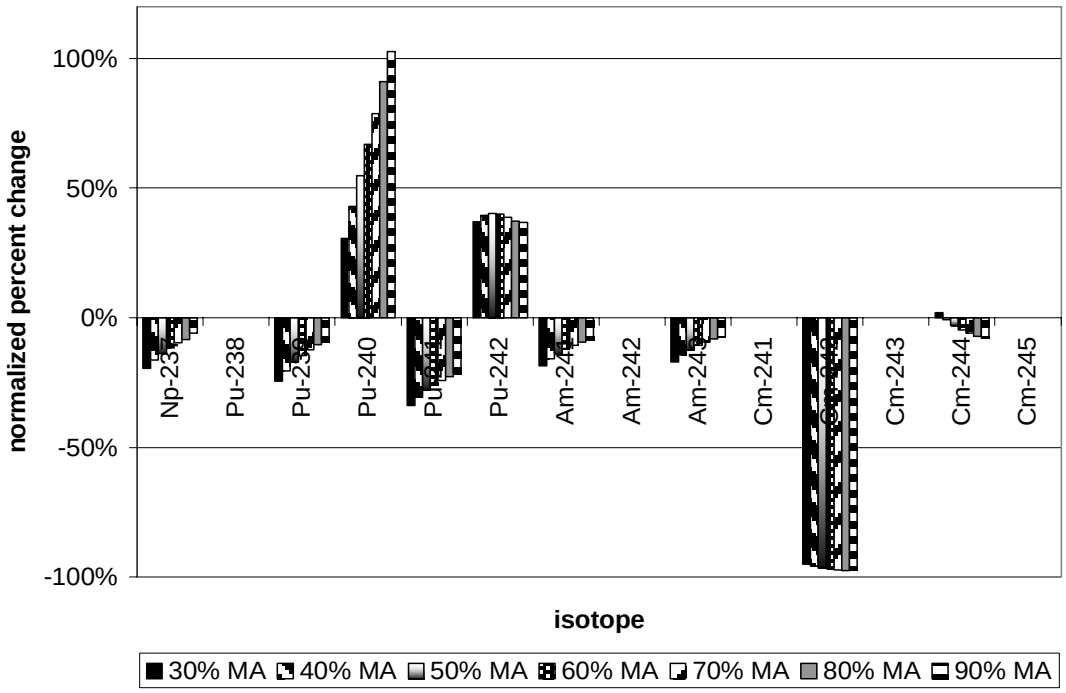

Fig. 19. Normalized plot of the effect of minor actinide percentage on burnup. Normal power (714MWth/core, 10.82 kW/pin), 1,080 day burn cycle.

Not shown is the corresponding decrease in ^{233}U bred into the fuel due to the smaller fraction of ^{232}Th as the minor actinide fraction is increased. However, when looking at the normalized change in percent with respect to the amount of material fed in (Fig. 19), an important point is demonstrated. Notice that the effect of increasing the minor actinide fraction of the fuel decreases the overall transmutation efficiency. If 30% MA is in the initial fuel, then, for example, ^{241}Am changes -18.5%. If the minor actinide concentration is 90%, the change in the amount of ^{241}Am is -8.59%, or less than half as much, percentage wise, even though three times the initial amount is fed in. 2.59 grams of ^{241}Am are burned in the 30% MA pin versus 3.52 grams in the 90% MA pin. So for the additional reprocessing problems and worse delayed neutron fraction, not much is

gained from increasing the minor actinide fraction. This is a disappointing result. Then again, with 169 pins per assembly, it would only take less than 7 full assemblies of 90% MA fuel versus 30% MA fuel to burn more than an extra kilogram of ^{241}Am. The issue at this point becomes more of an optimization question. What is the main priority from a repository standpoint?

Delayed Neutron Information

The delayed neutron fractions for these fuels are shown below in Table 10. As can be seen, the delayed neutron values for these pins are smaller than those for normal MOX LWR pins, which were in the 0.0030-0.0040 range. This has additional implications regarding control of a reactor using these fuels. However, although this is an issue that must be accommodated in the core design and control strategy, it is important to remember that the entire core will not be fueled with these transmutation pins. The total delayed neutron fraction of the reactor core is the weighted sum of contributions from all the isotopes in the entire core. Therefore, when these fuels are placed into the reactor, this delayed neutron fraction creates a limit to the amount of normal fuel assemblies that can be replaced with transmutation assemblies, but would not prevent their use. As can be seen in the above table, the presence of thorium does increase the delayed neutron fraction, but it still has a smaller delayed neutron fraction than normal MOX fuel. For burning minor actinides in a dedicated fast reactor system, in which these fuels would be a large component of the core, however, using thorium significantly increases the safety margin relative to the higher MA fuels.

Table 10
Delayed neutron values for the minor actinide nitride MONJU pins

Run	MA	Pu	β
2Mpin41	30%	7.6%	0.002681
2Mpin42	30%	6.0%	0.002693
2Mpin43	30%	4.5%	0.002712
2Mpin44	40%	7.6%	0.002404
2Mpin45	40%	6.0%	0.002400
2Mpin46	40%	4.5%	0.002398
2Mpin47	50%	7.6%	0.002189
2Mpin48	50%	6.0%	0.002176
2Mpin49	50%	4.5%	0.002164
2Mpin51	60%	7.6%	0.002015
2Mpin52	60%	6.0%	0.002000
2Mpin53	60%	4.5%	0.001981
2Mpin54	70%	7.6%	0.001874
2Mpin55	70%	6.0%	0.001856
2Mpin56	70%	4.5%	0.001836
2Mpin57	80%	7.6%	0.001755
2Mpin58	80%	6.0%	0.001738
2Mpin59	80%	4.5%	0.001718
2Mpin61	90%	7.6%	0.001640
2Mpin62	90%	6.0%	0.001639
2Mpin63	90%	4.5%	0.001620

In addition, as previously discussed, the higher MA fraction is actually not that much more helpful in increasing the transmutation efficiency of the minor actinides, and so therefore using thorium as the fertile diluent in the fuel helps increase the safety margin of these fuels, as predicted, both by increasing the delayed neutron fraction and by encouraging the use of the lower MA fuels.

Fertile Free Fuels

Next, some fertile-free fuels were modeled, with very high minor actinide concentrations. There is no uranium or thorium in these fuels initially. These fuel compositions are listed in Table 11, and use only minor actinide mixture #2.

Table 11
Fertile free fuel compositions

Run	MA	Pu	Np	β
3Mpin1	85%	5.0%	10.0%	0.001747
3Mpin2	85%	7.5%	7.5%	0.001739
3Mpin3	85%	10.0%	5.0%	0.001741
3Mpin4	90%	5.0%	5.0%	0.001639
3Mpin5	90%	7.5%	2.5%	0.001637
3Mpin6	90%	10.0%	0.0%	0.001638
3Mpin7	95%	0.0%	5.0%	0.001526
3Mpin8	95%	2.5%	2.5%	0.001529
3Mpin9	95%	5.0%	0.0%	0.001533

A plot of their k_{eff} values over burnup is given in Fig. 20. As can be seen, the reactivity increases quite a bit over the burnup, even though all of these pins start off with very high k_{eff} values. These pins are much more reactive than even the normal MONJU outer core MOX pin, and their delayed neutron fractions are smaller. This changes the control strategy for their use in the reactor.

If these fertile free compositions were to be used, they would have to be used in very small amounts and the whole core would have to be changed to accommodate the power spiking from these very reactive fuels. In addition, the delayed neutron values for fertile free fuels are very small, as shown above in Table 11.

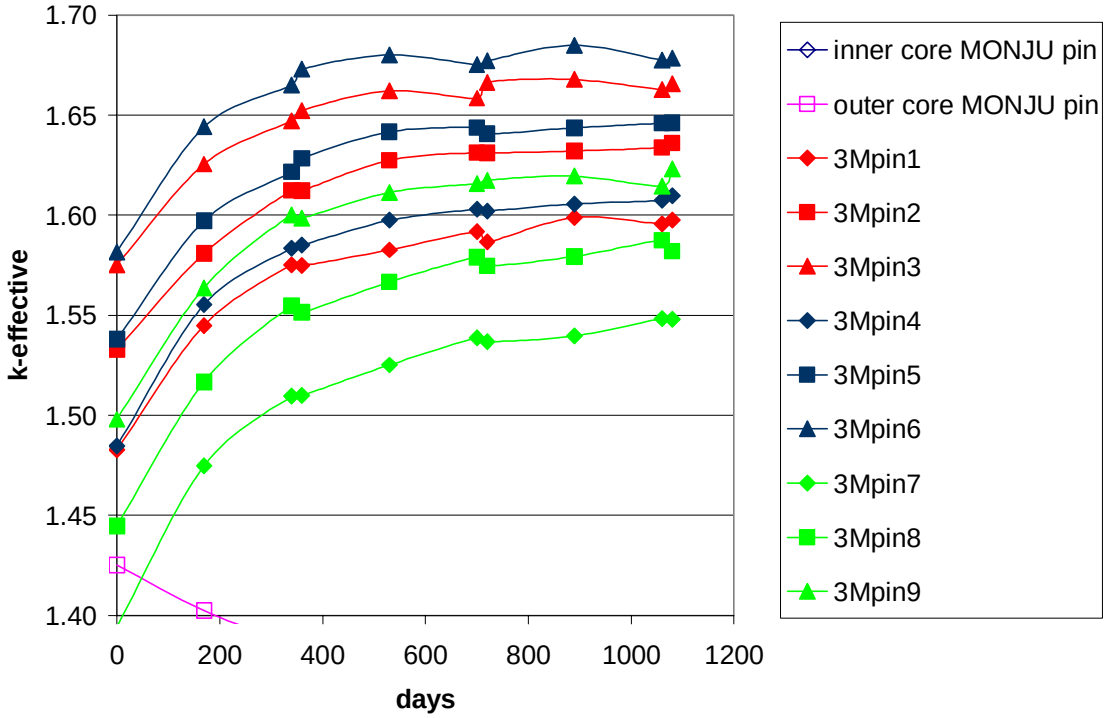

Fig. 20. k_{eff} values for the fertile-free nitride MONJU pins.

The change over burnup in the amount of material in the fertile free pins is what is interesting, or rather, not interesting about these plots. It would be assumed that fertile free pins would transmute much more material than was created. However, by using thorium, the only material that is created is ^{233}U and some of the plutonium isotopes, and this is shown in Fig. 21 with the fertile free results. The buildup of ^{233}U is not shown, but it will be given in the whole core section to determine the total amount of material produced. For the elimination of minor actinides, ^{233}U is not quite so important. These results resemble almost exactly the higher MA thorium-containing fuels. This is interesting, but the difficulty of controlling these fertile free fuels is their main drawback, with an inert matrix fuel form or any other such as this nitride fuel. It is

therefore preferable to use thorium as a fertile component, and when the whole core analysis is discussed it will be compared to the use of uranium as a fertile diluent in the fuels. These fertile free fuels will not be used in the whole core models.

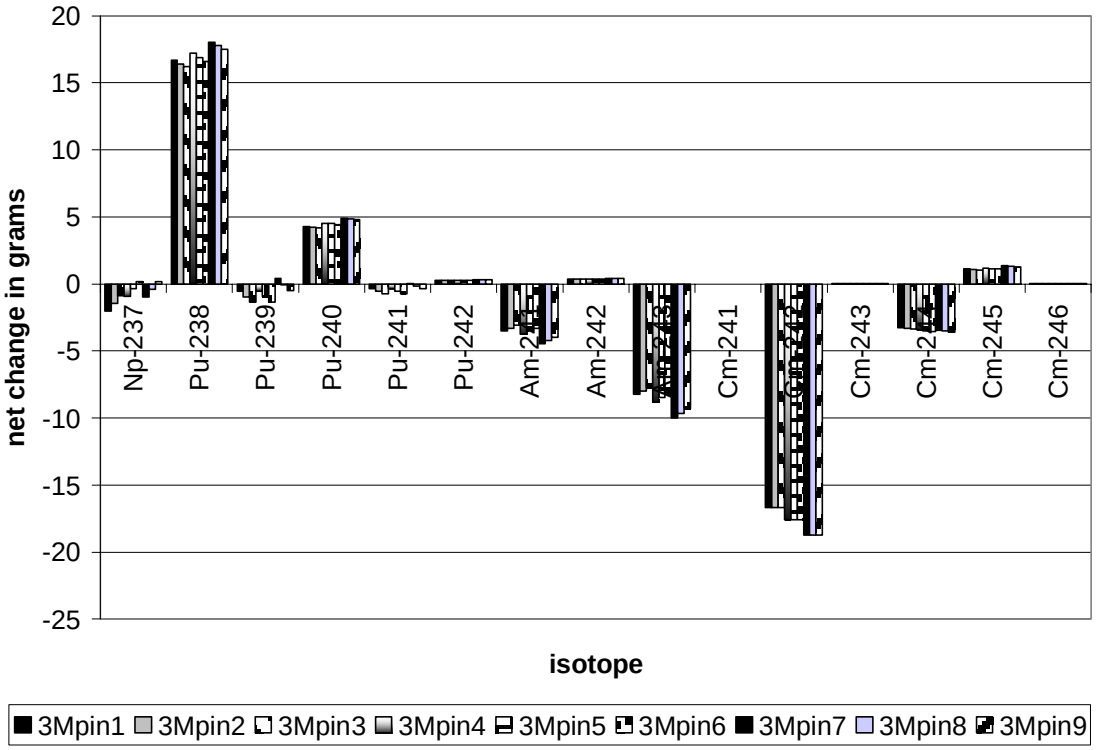

Fig. 21. Fertile-free fuel pins over 1,080 day burnup.

Temperature Calculations

The main advantage to be gained from using nitride fuels is twofold. First of all, since all of the actinides form mononitride compounds, there is only one atom of nitrogen per molecule for every atom of actinide, as opposed to the two oxygen atoms in the dioxide compounds. This means a higher heavy metal density in the fuel and thus more heavy metal can be put into the same fuel volume. However, the real advantage in

using nitride fuels instead of oxide fuels is that they have a much higher thermal conductivity, and therefore for the same power, the fuel temperature will be lower. This means that the power density can be increased without raising the temperature of or damaging the fuel [27].

For example, fuel centerline temperature of the MONJU core is 1058°C. (I have calculated 951°C, but that doesn't take into account the power distribution over the core). The thermal conductivity of UO_2 fuel at 1000°C temp from Todreas and Kazimi is 0.029 W/cm-K, and from Y. Arai et al., the thermal conductivity of UN is on the order of 0.20-0.25 W/cm-K for the same temperature [22,28]. This is about 10 times as large. The melting points for UO_2 and UN are about the same, 2730°C versus 2600°C. For PuO_2 and PuN they are slightly less, or 2300°C and 2500°C, respectively [27]. Therefore, for the same fuel centerline temperature, nitride and oxide fuels both operate quite far below their melting points. However, by using nitride fuel, the power density can be greatly increased, as much as by a factor of 2, and still have about the same fuel centerline temperature. This is very advantageous, because much higher burnups can be achieved in the same amount of time in-core. Table 12 displays some of the temperature data for MONJU pins, oxide versus nitride.

There is a drawback in that this data is for (U,Pu)N and not for minor actinide nitrides. Using it is a most likely incorrect approximation. However, no data could be located for AmN and CmN, and none is identified by Thetford and Mignanelli [29]. The tendency for (U,Pu)N is that the thermal conductivity decreases as the Pu content goes up, and the thermal conductivity for NpN is between that of UN and PuN. So to use this

thermal conductivity information is not really appropriate for these fuels, but it is a better approximation than using data for oxide fuels. Therefore, a value of 0.2 W/cm-K has been used to calculate the data found in Table 12. The thermal conductivity of thorium nitride also could not be located. The thermal conductivity of thorium metal is twice that of uranium metal, but data on the compound is unavailable.

Table 12
Fuel centerline temperature comparison for oxide fuels versus nitride fuels

Core Power, MWth	T_{CL}, Oxide °C	T_{CL}, Nitride °C	Power Density, W/g
714	951	714	121
814	1029	758	138
914	1106	802	155
1014	1184	847	172
1114	1261	891	189
1214	1339	936	206
1314	1416	980	223
1428	1505	1031	242

In light of the higher thermal conductivity of nitride fuels, some of the best pins that were modeled using the standard MONJU power density of 121 W/g were run again, with a doubled power density. This corresponds to a whole core power of 1428 MWth, as listed in the last line of Table 12 above. The k_{eff} values for these pins, given in Fig. 22, are almost exactly the same as those of the second minor actinide mix above. In fact, the only difference is the doubled power level of the burn of these pins, so this is not a very surprising result. However, it seems that the values should be slightly different since at least in theory more material is being transmuted over the same burn cycle since the power level is twice that of the first pins.

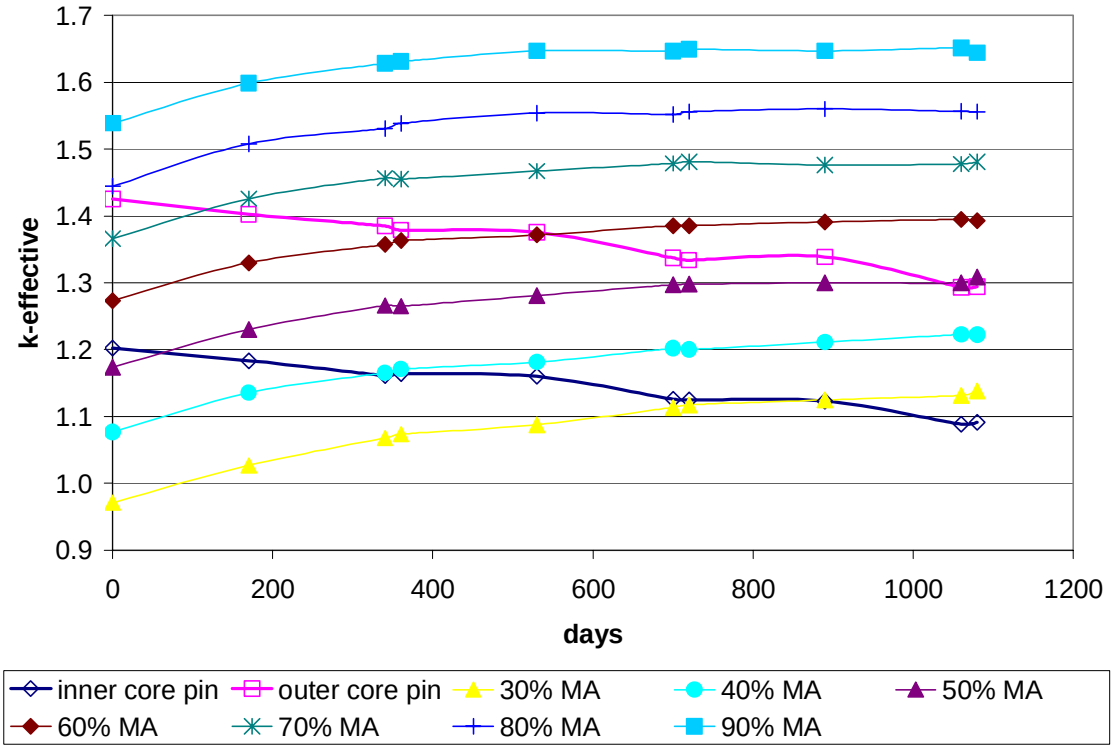

Fig. 22. k_{eff} values of the increased power MONJU transmutation pins

Therefore, it is important to look at the concentrations of the various isotopes and compare them to the normal power runs. The transmutation of neptunium, plutonium, americium and curium are shown in Fig. 23 and Fig. 24 for the normal and double power runs.

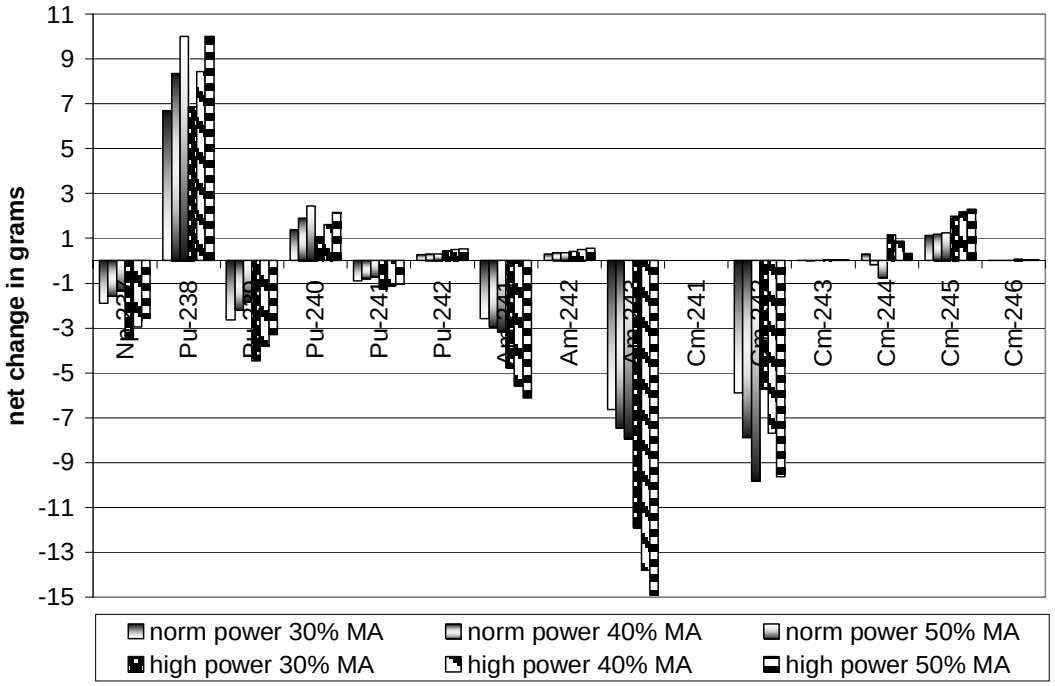

Fig. 23. Comparison of the transmutation of 30-50% MA fuels with increased power.

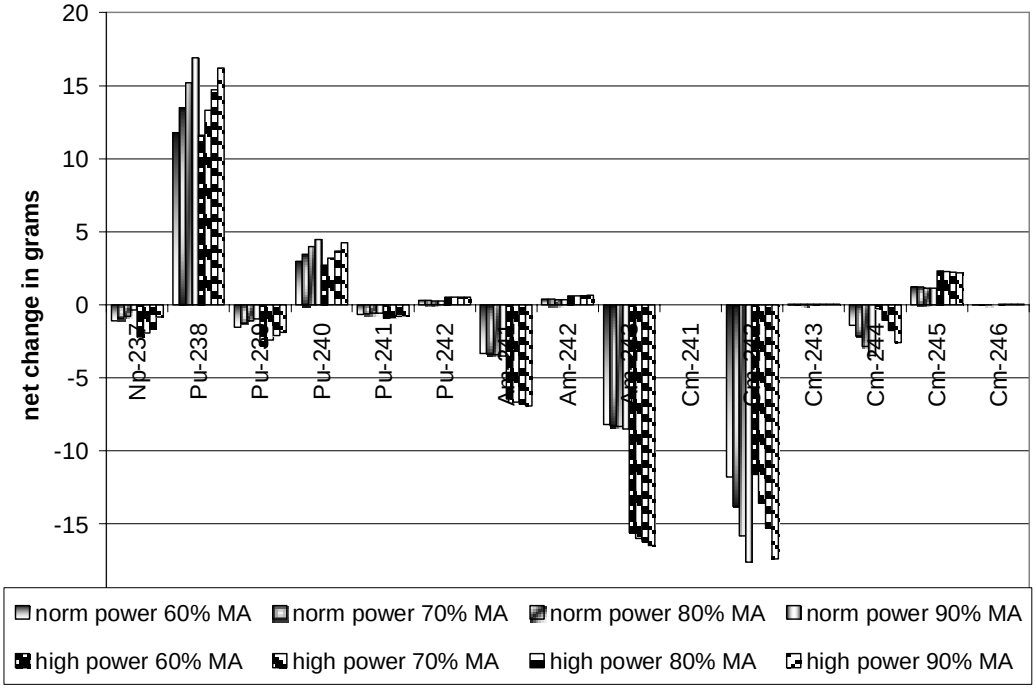

Fig. 24. Comparison of the transmutation of 60-90% MA fuels with increased power.

As can be seen, we do find that a great deal more material is burned by doubling the power. Such a large power increase might not be possible, unless the whole core was loaded entirely with transmutation fuel. But as the fraction of nitride fuel in the core goes up, the power may hopefully be correspondingly increased. The oxide fuels have to be taken into consideration, because although the nitride fuels will be fine, the oxide pins will increase their centerline temperature as shown above in Table 12.

One interesting thing to note is that while some isotopes are transmuted much more, notably ^{237}Np, ^{239}Pu, ^{241}Am, ^{243}Am, and ^{245}Cm, the burnups of all other isotopes don't change with respect to the increased power. This is likely the result of the complicated interdependent series of radiative capture reactions, fissions, and decays creating and destroying the same isotopes to give the balances shown in the plot.

Another interesting effect is the transmutation of ^{244}Cm, which for normal power turns negative at 40% MA concentration, but for double power stays positive until the concentration of minor actinide builds up to 60%. This discrepancy can probably be explained by the following reaction:

$$^{243}Am + n \xrightarrow{78\text{ barns}} {}^{244}Am + \gamma \xrightarrow{10.1\text{ hours}} {}^{244}Cm + \beta^- \tag{3.3}$$

or by the following reactions, from ^{242}Am, which also helps explain the growth of ^{242}Pu:

$$\begin{array}{l} {}^{242}Am \dfrac{\xrightarrow{16.02\text{ hours, }82.7\%}}{+\beta^- \quad \xrightarrow{17.3\%}} \dfrac{{}^{242}Cm + \beta^-}{{}^{242}Pu} \\ {}^{242}Cm + n \xrightarrow{20\text{ barns}} {}^{243}Cm + \gamma + n \xrightarrow{130\text{ barns}} {}^{244}Cm + \gamma \end{array} \tag{3.4}$$

Noticing the rate at which ^{241}Am is transmuted with respect to the percentage of minor actinide, the amount of increase in transmutation of this isotope is decreasing as the minor actinide fraction goes up in Fig. 23, By comparing it to Fig. 24, the decreasing

rate of the increase of ^{241}Am transmutation can especially be seen. This means that the balance equation for the rate of change of ^{244}Cm, given as equation 3.5, has a negative left side now and the total amount decreases over the burnup if there is enough minor actinide in the fuel to slow down the breeding from ^{244}Am and ^{243}Cm.

$$\frac{dn^{64}}{dt} = \sigma_{\gamma}{}^{63}\phi n^{63} + \lambda^{54\to 64} n^{54} - (\lambda^{64} + \phi\sigma_a^{64}) n^{64} \tag{3.5}$$

where

n^i = concentration of isotope i at time t
σ_γ^i = microscopic (n,γ) absorption cross section for isotope i
ϕ = scalar flux at time t
$\lambda^{i\to j}$ = decay constant for isotope i to isotope j
λ^i = decay constant for all decay of isotope i
σ_a^i = microscopic absorption cross section for isotope i

In this equation the isotope is written with the first number representing the last digit of Z and the second number representing the last digit of A. The number 64, for example, corresponds to $^{244}_{96}$Cm [25].

The normalized percent change plots are not given, because they are not very interesting. We have already shown above that a greater percentage of the fissile isotopes have been burned, since the starting material is the same but was used to produce double the power. Since the material is the same, $Q_{fission}$ will be the same (at least at the beginning before the composition of the fuel changes) and therefore, logically, to get twice the power we need twice the number of fissions to produce that power. What is interesting is where those fissions come from, and how the burnup of isotopes changes other than doubling. For the most part, they don't. This is a good

result, supposing that in the whole core loading enough nitride fuel in to increase the power sufficiently and benefit from the increased thermal conductivity of the nitride fuel. Otherwise, it will simply be a fuel with a wide margin of safety since the temperature will be well below that of the oxide fuel in the core. This will be looked at in greater detail upon discussing the whole core simulations.

Whole Core Calculations

The first thing to do when determining where to load transmutation fuel into the MONJU core requires thinking about the flux profile of the core as it is loaded with standard MOX pins. It would be advantageous to put the transmutation fuel in locations with a high neutron flux in order to increase the number of capture and fission reactions in the transmutation fuel from the large population of neutrons in those areas. Then again, it would also be advantageous to put these highly reactive fuels into regions of low neutron flux, to get the power profile flatter over the core. In the end, the fuels also have to have relatively similar k_{inf} values (as modeled in the single pin infinite lattice simulations) so that the core will be as close to the existing standard model as possible, despite being fueled with transmutation fuel.

In addition, there is another consideration as discussed in the last section with regard to the power of the core. To take advantage of the ability of nitride fuel to operate at higher power due to its increased thermal conductivity, and also to transmute as much fuel as possible, it is desirable to load as much of the core as possible with nitride transmutation fuels. If possible, the best case scenario would involve loading the entire core with (Th,An)N fuels, but this will prove difficult because the axial and radial

blanket regions of the core have very low reactivity since they are designed and placed in the core to capture neutrons and breed plutonium. All of the minor actinide nitride fuel pins modeled are very reactive, more so even than the 16% plutonium-fueled inner core region. However, the thermally hotter regions of the reactor are in the inner and outer core, because that is where all the fission is taking place, and therefore it is more crucial to replace the inner and outer core MOX regions with nitride transmutation assemblies.

In addition, MONJU is a relatively small core. The initial fuel loading for the whole core is around 30 tonnes of fuel, and the PWR modeled in this study has an initial core loading of 90-100 tonnes of fuel. It is desirable to load it with as much transmutation fuel as possible, since even with full-MA cores it would likely take a large amount of new MONJU-sized reactors to transmute the spent nuclear fuel inventory of the United States. Depending on the number of thermal transmuters and the length of time desired to achieve a closed fuel cycle, at least 5-10 MONJU-sized fast transmuters would be necessary. This is the topic of chapter IV.

The first calculations performed for the whole MONJU core involved replacing the inner core of MONJU with 30% MA thorium nitride fuel, and replacing the outer core with 50% MA fuel. This provided a k_{eff} value of roughly 0.8 at BOL and ~0.9 after 1 year. For the next MONJU case, the inner core was loaded with 30% MA and the outer core with 60% MA. This was satisfactory from a reactivity standpoint, with k_{eff} rising to almost critical after one year of burn. With some small adjustments it could probably be used. However, this core loading continued to breed plutonium in the

depleted uranium blanket. This is undesirable since the objective is to transmute plutonium as well as minor actinides. If the depleted uranium blanket fuel is retained, no progress has been made in reducing the overall inventory of plutonium with the fast system transmuter.

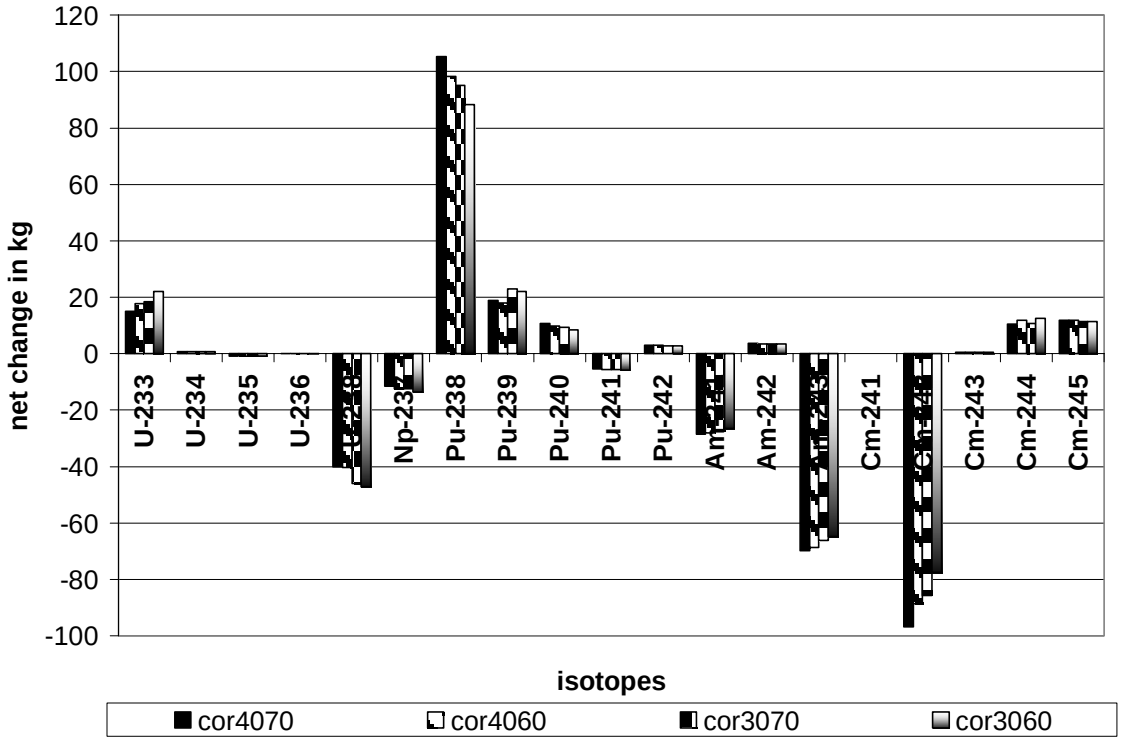

Fig. 25. MONJU whole core calculations, indicating the necessity of removing the depleted uranium blanket.

For the first series of whole core tests the blanket was not changed, and these results, given in Fig. 25, demonstrate the need to replace the DU blanket with some MA fuel of low reactivity. This will also enable the investigation of the impact of using a whole core of MA fuel. It will still produce plutonium, but the hope is that both less

plutonium will be created than in this core and that it will be less attractive from a proliferation standpoint. Most of the plutonium being produced is ^{238}Pu and ^{240}Pu. The ^{239}Pu will be burned as long as the blanket does not produce more than is consumed. Unfortunately, it will likely have a low delayed neutron fraction due to the (Th,MA)N-fueled core.

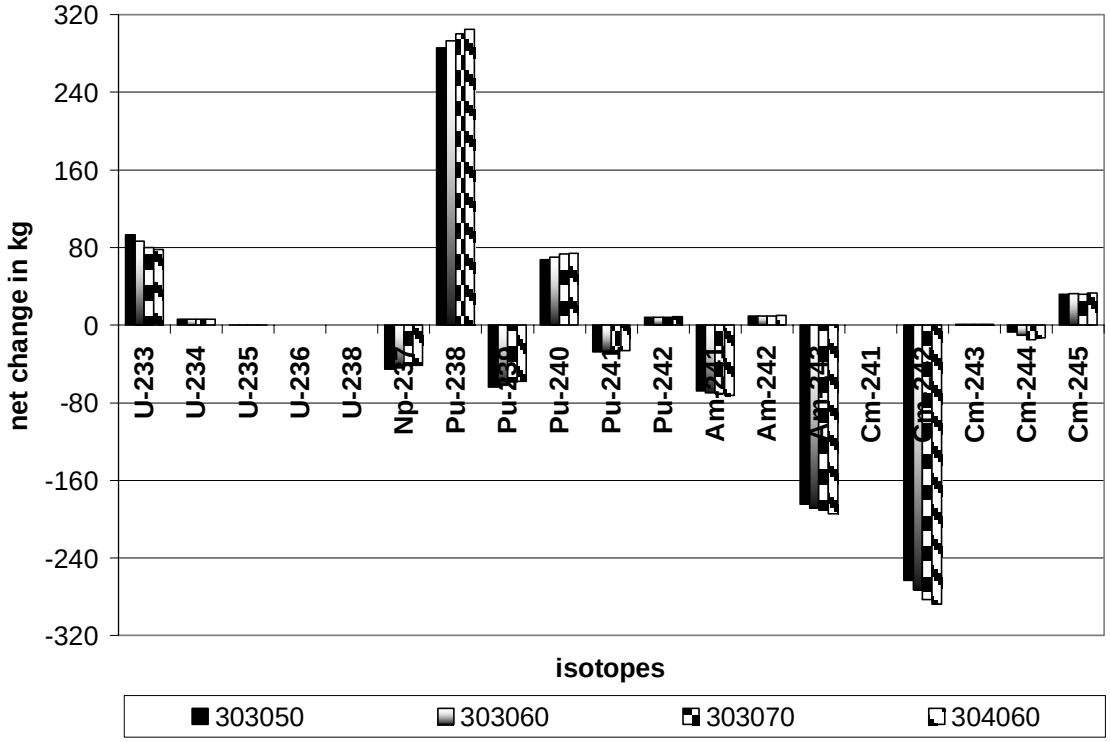

Fig. 26. Transmutation of MONJU whole cores using 30% MA fuel as blanket.

The next calculations performed replaced the depleted uranium blanket areas in the MONJU core, both radially and axially, with 30% MA fuels. As can be seen in Fig. 26, this leads to a great deal of plutonium being created, despite the burnup of the fissile ^{239}Pu and ^{241}Pu. Obviously, in this case, the source is not the depleted uranium blanket.

A possible explanation for this result is that the plutonium is being produced from the whole complicated Th,U buildup/decay chain, given in Fig. 27 [30].

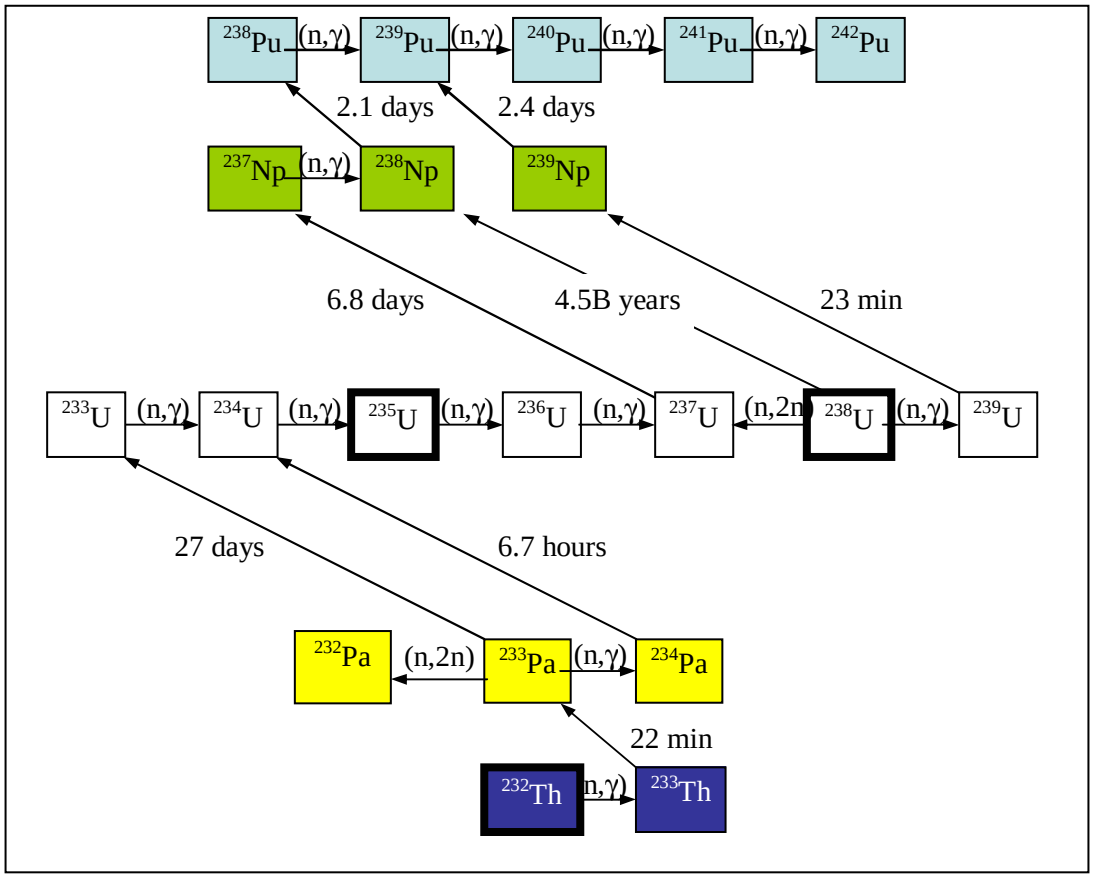

Fig. 27. Buildup/depletion chain for elements 90-94 (thorium through plutonium).

A good way to determine where the plutonium is coming from is to replace the thorium with uranium, and repeat the calculations. This buildup path is verified by the results of these repeated calculations, as shown below in Fig. 28. The only sources for the plutonium are the buildup through thorium, or the alpha decay of ^{242}Cm, which is in fact where most of the plutonium is likely to come from, but the remainder is created

from the thorium. ^{242}Cm is a more likely source because there are several isotopes that are created through buildup from thorium for which fission is more than absorption. The other reason is that a lot of ^{242}Cm has been used up, and its fission and capture cross sections are both rather small. Therefore, most of the ^{238}Pu comes from ^{242}Cm. The addition of thorium didn't change the results very much for the fast reactor system.

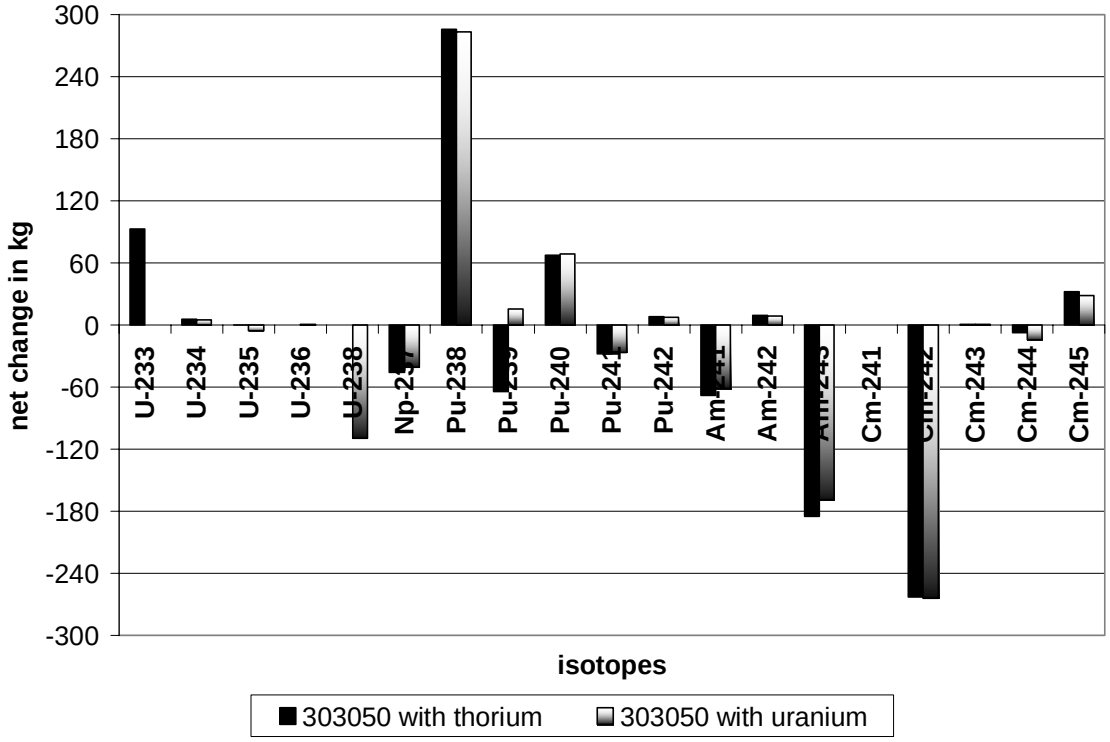

Fig. 28. Difference between thorium and uranium as alloying agent for MA fuels.

This is not very surprising. The main advantage of using thorium is that later, upon multiple recycle, the thorium-MOX fuel that will be put into the thermal reactor system helps burn more plutonium than the normal MOX fuel. This was not addressed

in Chapter II, because that was meant to reflect both the current DOE recycling strategy, and also the first stage in this study's closed fuel cycle. Therefore, analysis was performed for the plutonium transmutation rate based on recycle back into the thermal transmutation systems.

Thermal Transmutation of Fast Reactor-Produced Plutonium

The analysis of putting the fast reactor-burned MA fuels depends on a few factors. First of all, the core loading of MONJU is much less than that for a whole PWR core, but the actinide loading in the entire MONJU core is very similar to the 32% MOX part of the PWR core (29 tonnes versus 27). Therefore, the analysis presented below compares the 1/3 MOX fueled core with 4% neptunium transmutation rate to a PWR in which the 1/3 MOX assemblies are replaced with the whole core of spent thorium/minor actinide nitride fuel from the MONJU core.

The MONJU spent fuel came from the run with the 30% MA blanket, 30% MA inner core and 50% MA outer core fuels. Fig. 29 and Fig. 30 below show the results of this cycle. These figures represent the oldest regular fuel and the MOX fuel after three cycles (i.e., the yearly discharge from the core).

The percent change in each of these isotopes normalized to the amount in the feed is given below in Fig. 30. The transmutation of plutonium in the MONJU-fueled transmutation PWR shows similar results. This is a disappointment. Also not shown is the difficulty in reprocessing spent MONJU fuel for reinsertion into the thermal systems. Nitride fuels cannot be used in water-cooled reactors, because if the cladding is breached

the fuel will oxidize and the increased volume of the fuel after oxidation will cause the fuel to swell and rupture, dispersing the fuel material throughout the coolant.

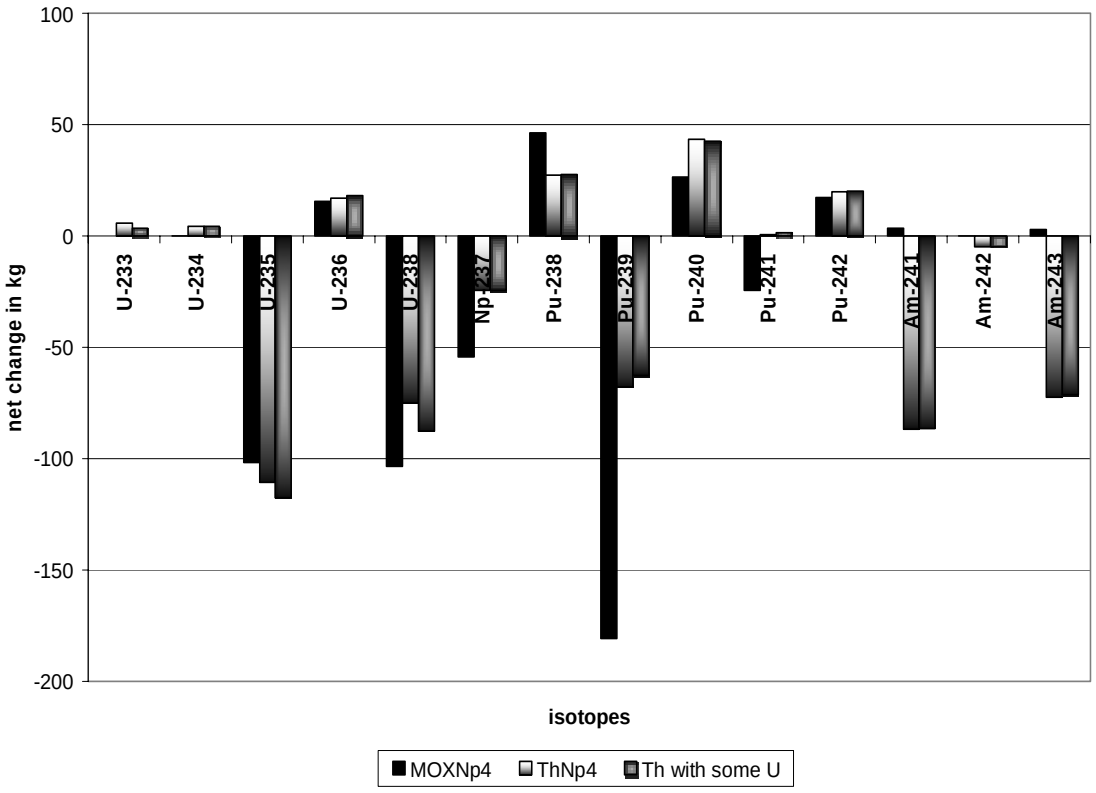

Fig. 29. Net change in kilograms per year for whole PWR cores, 1/3 fueled with either MOX or spent MONJU transmutation fuel after 1,080 days burn.

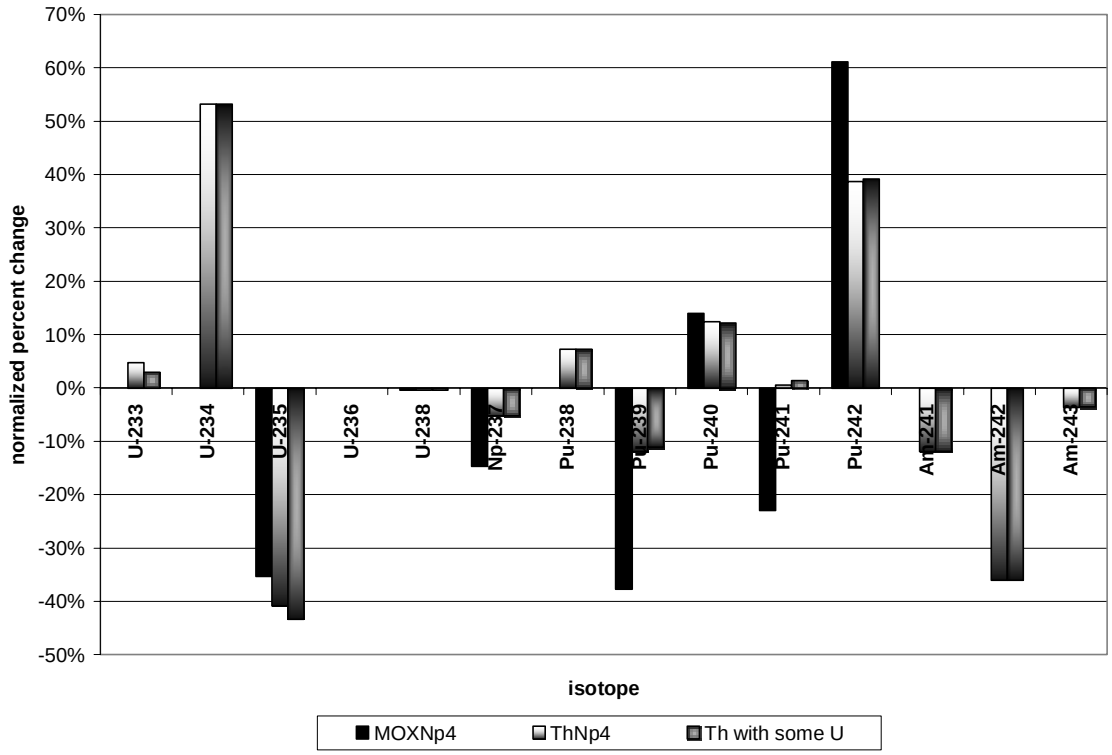

Fig. 30. Normalized percent change of MOX PWR core versus MONJU spent fuel core.

Results obtained with the addition of a small amount of ^{238}U were about equal. Although avoiding ^{238}U in a transmutation system is one of the focuses of this study, the proliferation resistance of the fuel is also important, and when ^{233}U is produced from thorium, without ^{238}U, it is very easy to separate chemically from the other elements in the spent fuel. ^{233}U by itself makes an excellent weapon material. The addition of some ^{238}U can mitigate this threat. It has been suggested by Forsberg et al. that for uranium mixtures, non-weapons-usable uranium can be defined by equation 3.6 [31].

$$\frac{\text{weight } {}^{233}\text{U} + 0.6*(\text{weight } {}^{235}\text{U})}{\text{weight of total uranium}} < 12\% \qquad (3.6)$$

For the mixture given in Fig. 30, the value given by this equation is only ~1.1%.

Chapter Summary

In this chapter the transmutation capabilities of nitride fuels containing large quantities of minor actinides with thorium as the fertile diluent were examined. These fuels were put into a reactor system with a fast neutron spectrum, and proved to transmute large quantities of minor actinides. However, the buildup of various plutonium isotopes, particularly ^{238}Pu and ^{240}Pu, can be counterproductive. Plutonium burning is the focus of the Series I fuel transmutation scheme, which utilizes thermal spectrum reactors to burn plutonium. These isotopes can in fact be transmuted in thermal transmutation systems, but not as readily as the fissile isotopes. However, the presence of ^{240}Pu especially decreases the proliferation risk of the plutonium in these fuels, which is another priority for the Advanced Fuel Cycle Initiative. On the subject of proliferation, with the addition of a small amount (6%) of ^{238}U to the MA fuel, the proliferation resistance of thorium-containing fuel can be increased without much change on the transmutation rates. The best of all these results will be used in Chapter IV, to determine how many fast reactors are necessary to transmute the spent nuclear fuel inventory of the United States using this two tier transmutation scheme.

CHAPTER IV

CLOSING THE FUEL CYCLE

Introduction

The obvious main drawback to the transmutation of spent nuclear fuel in a reactor system is that during the burn cycle, potentially more material is being generated in the entire inventory of nuclear plants. In the first stage of any program to "deal with America's nuclear waste problem," it is necessary to burn more plutonium and minor actinides than is created in order to reduce the stockpile of nuclear waste destined for Yucca Mountain. However, nuclear power is not diminishing. To the contrary, the future of nuclear power for electricity generation and even for hydrogen production is promising. Therefore, it is desirable to seek at least equilibrium in which there are enough transmutation systems to reduce the current inventory of nuclear waste to fit into the Yucca Mountain Repository, and then to balance the waste that is being produced and will continue to be produced in our commercial reactors. The benefit of using reactors as opposed to accelerator-driven systems for waste transmutation is that after the waste stockpile has been reduced to an acceptable level, the fuel used in the transmuter reactors can be changed to keep the waste inventory at this level. Then the transmutation reactor systems will be the last step in a closed fuel cycle that produces electricity and handles its own waste.

Below, Fig. 31 shows the statutory and theoretical capacities of the Yucca Mountain Repository, and the projected spent fuel inventory past 2040 without

reprocessing/transmutation, and with the result of implementing the Advanced Fuel Cycle Initiative transmutation program [32].

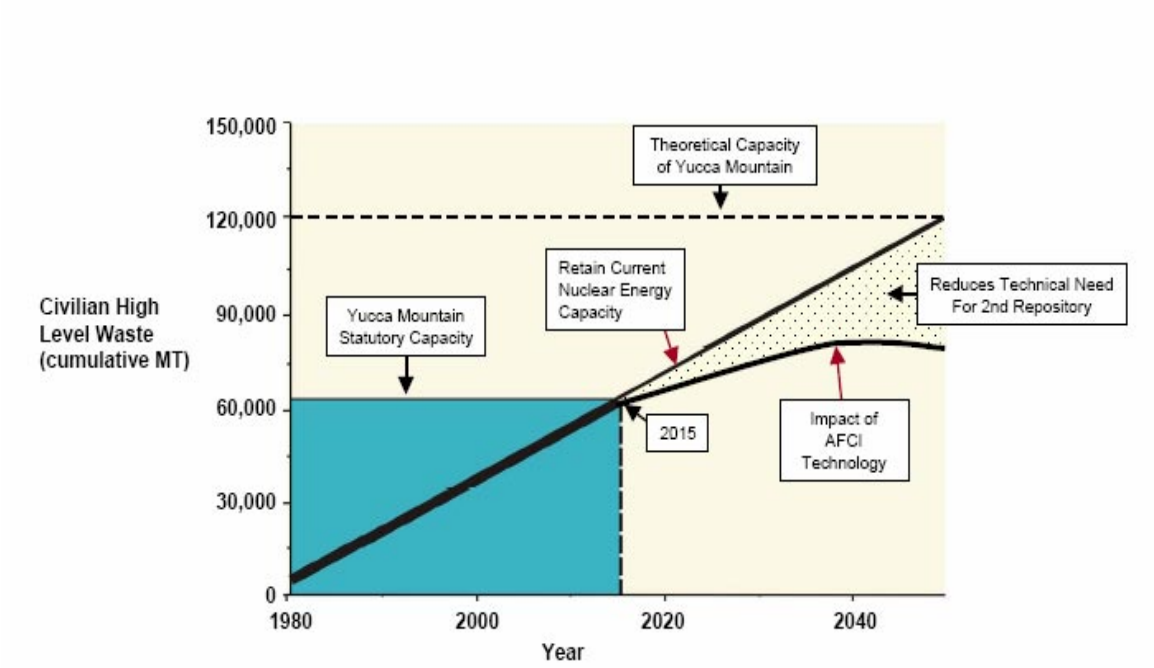

Fig. 31. Projected spent fuel inventory with and without AFCI transmutation program.

Methodology

The current US stockpile of spent nuclear fuel is approximately 40,000 tonnes, as of 2001, and each year about 2,000 tonnes are produced from the existing fleet of reactors [25]. The following balance equation determines when equilibrium will be achieved, or when more material is transmuted more than is produced.

$$SNF = \sum_i \left(L_i + n_i \right) \tag{4.1a}$$

$$\sum_i n_i = \sum_i \left(yN_C I_i^C P_i^{prC} + yN_{thT} I_i^C T_i^{thT} + yN_{fsT} I_i^C T_i^{fsT} \right) \tag{4.1b}$$

where

$SNF =$ the total spent nuclear fuel inventory
$L_i =$ the legacy amount of isotope i from the stockpile
$n_i =$ the net amount of isotope i produced in y years
$y =$ the number of years of transmutation
$N_C =$ the number of commercial reactors
$I_i^C =$ the initial core loading of isotope i
$P_i^{prC} =$ the yearly production rate of isotope i in commercial reactors
$N_{thT} =$ the number of thermal transmuter reactors
$T_i^{thT} =$ the yearly transmutation rate of isotope i in PWR transmuters
$N_{fsT} =$ the number of fast transmuter reactors
$T_i^{thT} =$ the yearly transmutation rate of isotope i in fast transmuters

Equilibrium with the current legacy spent fuel stockpile, of course, would be reached if n_i reaches zero. If the goal is to reduce the amount of spent fuel in the stockpile, then the number of transmuter reactors must be increased to make n_i greater than zero, so that the total amount of spent fuel decreases to whatever the desired level.

These equations give the net production of spent fuel. Currently, the number of thermal and fast transmuters, N_{thT} and N_{fsT}, are zero and so n_i equals 2 million kilograms of spent fuel produced per year. The total inventory is the legacy plus the current yearly production with no transmutation. It is desired to stabilize or decrease SNF. L_i is known, as are N_c and P_i^{prC}. The transmutation rates of thermal and fast transmuters have been determined through this study in chapters II and III, and are summarized in Table 13.

Interesting things to note in Table 13 are that the total amount of material burned in a PWR is significantly less than in the transmutation PWR cores. This is because the transmutation values are for the three-times-burned UO_2 and the transmutation fuel, and

the sum of these fuels is a larger fraction of the core and therefore more material than in the normal one PWR (~55% versus 32%).

Table 13
Transmutation rates (net change over 1 year for the last year of a 3 year burn cycle) by isotope for the systems chosen in chapters II and III

	Thermal				Fast		
Isotope	PWR	0% Np	0.04% Np	4% Np	70outer	Du3060	60outer
^{232}Th	0	0	0	0	-17.700	-82.200	-11.000
^{231}Pa	0	0	0	0	0.198	0.728	0.135
^{233}Pa	0	0	0	0	0.603	2.520	0.367
^{232}U	0	0	0	0	0.039	0.172	0.026
^{233}U	0	0	0	0	12.000	53.167	7.467
^{234}U	0.009	0.009	0.070	0.507	1.370	3.634	1.386
^{235}U	-241.333	-145.700	-135.600	-112.300	-3.514	-2.125	-3.331
^{236}U	33.656	22.900	21.200	17.270	0.783	0.525	0.745
^{238}U	-256.667	-202.400	-181.800	-187.600	-236.667	-131.000	-221.000
^{237}Np	2.520	1.594	-18.367	-164.486	-11.697	-33.727	-11.207
^{238}Pu	0.872	0.941	17.023	139.046	62.328	112.691	69.975
^{239}Pu	12.030	-667.560	-618.656	-540.899	82.767	66.567	79.900
^{240}Pu	17.044	53.380	56.300	62.450	14.703	25.613	17.110
^{241}Pu	5.867	-86.882	-81.725	-75.860	-22.890	-12.969	-21.997
^{242}Pu	9.478	60.620	55.480	48.280	4.127	6.514	4.437
^{241}Am	0.144	8.804	9.319	9.779	-34.382	-66.366	-39.235
^{242}Am	0.001	0.082	0.086	0.087	3.893	6.663	4.323
^{243}Am	1.557	9.876	8.615	8.330	-90.053	-164.333	-101.467
^{241}Cm	0	0	0	0	0	0	0
^{242}Cm	0.119	1.625	1.445	1.347	-57.530	-99.333	-67.206
^{243}Cm	0.003	0.014	0.011	0.009	0.335	0.613	0.363
^{244}Cm	0.464	1.131	0.929	0.696	10.100	18.000	8.404
^{245}Cm	0.007	0.016	0.016	0.010	15.311	28.033	16.708
^{246}Cm	0.003	0.001	0.001	0.001	0.350	0.711	0.360
^{247}Cm	0	0	0	0	0.003	0.007	0.003
^{248}Cm	0	0	0	0	0	0	0.000
Total	-412.667	-941.55	-865.65	-793.33	-265.522	-265.200	-264.734

The initial core loadings will be added to the total, for fresh PWR fuel, and taken from the legacy spent nuclear fuel stockpile for transmutation assemblies. This reflects

the fact that commercial reactors will likely continue mining, enriching and using UO_2 fuel, but the transmutation cores will be used for transmuting the legacy spent nuclear fuel. The initial core loadings are given in Table 14. All isotopes above ^{244}Cm are zero as initial loadings and are therefore deleted from this table. These figures represent the transmutation cores, and for the PWR systems, 1/3 of the normal UO_2 fuel, since these are equivalent yearly loadings to match the yearly net discharges given in Table 13.

Table 14
Initial core loadings of fast and thermal transmutation systems, kilograms

	Thermal				Fast		
Isotope	PWR	0% Np	0.04% Np	4% Np	70outer	Du3060	60outer
^{232}Th	0	0	0	0	217.7	1326.7	336.7
^{231}Pa	0	0	0	0	0.0	0	0.0
^{233}Pa	0	0	0	0	0.0	0	0.0
^{232}U	0	0	0	0	0.0	0	0.0
^{233}U	0	0	0	0	0.0	0	0.0
^{234}U	0	0	0	0	0.0	0	0.0
^{235}U	394	449	448	321.5	15.2	13.2	15.2
^{236}U	0	0	0	0	0.0	0	0.0
^{238}U	29100	45500	45400	44500	7446.7	6433.3	7446.7
^{237}Np	0	0	111	1110	48.3	117.7	48.3
^{238}Pu	0	0	0	0	0.1	0	0.1
^{239}Pu	101	1299.8	1299.5	1299.5	200.7	131	201.0
^{240}Pu	27	530.6	530.5	529.5	83.3	54.4	83.4
^{241}Pu	10.1	306.98	306.95	306.95	48.4	31.9	48.4
^{242}Pu	0	85.3	85.3	85.2	14.0	9.1	14.0
^{241}Am	0	0	0	0	163.0	240.7	140.3
^{242}Am	0	0	0	0	0.0	0	0.0
^{243}Am	0	0	0	0	453.3	668.3	390.0
^{241}Cm	0	0	0	0	0.0	0	0.0
^{242}Cm	0	0	0	0	72.0	106.3	62.0
^{243}Cm	0	0	0	0	0.0	0	0.0
^{244}Cm	0	0	0	0	178.3	263	153.3
Total	29632.1	48171.68	48181.25	48152.65	8941.0	9395.6	8939.5

The rate of production of spent nuclear fuel from the commercial cycle is also given above in Table 13, and was calculated for a normal Westinghouse PWR with 3 fuel regions, fresh, once and twice burned, over a 360 day period. Therefore, the net amount of each isotope produced or destroyed per year will be the result for the twice burned fuel at the end of that year, because the rest of the fuel will be shuffled to new positions and remain in the core. The transmutation rates for the MOX cores reflect the sum of the net change in the MOX region over three cycles added to the net change for the twice-burned UO_2 region. This is basically the fuel that would reasonably be discharged every year from the reactor, i.e. three-time burned spent UO_2 fuel and three-time burned MOX transmutation fuel.

The MOX fuel used in calculating this data has been irradiated in the reactor for two full year cycles, so that the discharged UO_2 fuel and the discharged MOX have similar irradiation histories even though their burnups are different. The burnups are different because if more fission takes place in the more highly reactive MOX assemblies, they are producing a bigger fraction of the total power and thus achieve a higher burnup over the same time.

Similarly, the transmutation rates for the fuels in the MONJU core were calculated for the fuels after they had been in the reactor for 3 full year cycles. These values will give values more closely approximating an equilibrium cycle in which MA transmutation fuels are burned for three years and then removed, rather than reflecting a one-year transmutation cycle from its startup with fresh MA fuel.

There are 69 PWR's in the United States and 35 BWR's. MOX can also be used in BWR's, although the results will be different. For one reason, the flux spectrums are quite different in BWR's as compared to PWR's and so it is incorrect in approximating all US thermal reactors as PWR's. The spent fuel from a BWR is isotopically different, and also the total amount of fuel in one core loading is different. However, since this is only an approximation, and since this study modeled a PWR, the thermal transmuter system will consist of only PWR's with a 32% MOX core loading. The MOX fuel used will be one of the three compositions listed in Table 14. This means if all the US PWR's are used for transmutation, 69 thermal transmuter systems are currently available in the United States. This is unlikely at best. However, this is one of the variables that can be controlled, i.e. the number of transmuter reactors being used to deal with spent nuclear fuel.

All production (non-transmuter) reactors in this scenario are approximated as PWR's, which is also an approximation. However, it is helpful in order to get a general idea of how many fast reactor systems might be necessary. For example, with no transmutation systems, approximating all US reactors as 3411 MWth Westinghouse PWR's gave a production rate of ~3063 tonnes average per year for 25 years. The real value is around 2000 tonnes per year, and so the production rate was normalized by taking the production rates from the 104 PWR systems and multiplying by 0.653 to get a total production of 2000 tonnes per year. This is not quite accurate, and the isotopics of the spent fuel will not be correct, but it provides a useful estimate. This data more

closely approximates the data given in Fig. 31, and serves to compensate for the diversity of types and sizes of US reactors.

The purpose of this chapter is to demonstrate the challenge in achieving equilibrium, and approximately how many reactor systems (and/or how many years) it would take to even level off production of spent nuclear fuel and make n_i above equal to zero. There are many variables in this equation, and nearly all of them can be changed to reflect policy and economic decisions such as the number of dedicated transmuter systems.

The United States does not currently operate any fast reactors, and therefore the number of fast transmuter systems in this equation is speculation. The development of fast reactors will be needed, either as power reactors under the Generation IV plan or as dedicated transmuter reactors built for dealing with spent nuclear fuel. It would of course be useful to produce power with the fast transmuters, as even older designs like MONJU have been shown (in this study at least) to be capable both of transmuting spent nuclear fuel as well as producing power. Economic factors will determine the final decision on this subject. However, the number of fast transmuter systems is another factor to be considered to see how effective these fuels are at transmuting both the waste being currently produced and the legacy spent nuclear fuel currently sitting in storage facilities.

Due to the lack of availability of these reactors at the present time, steps will be taken to keep the number of these systems as low as possible to make the calculations seem more realistic. Building 5 or 10 fast reactors for transmutation is within reason;

building 500 is not. The advantage of using these fast reactors systems is, of course, that per unit time and per kilogram of fuel, they can transmute far more minor actinides. This has the biggest impact over the long-term for a repository, and as a result fewer fast than thermal transmuters should be needed. It is important to remember that potentially the total spent fuel inventory can be reduced further by removing the ^{238}U from the waste. This may be a viable option because removing the bulk of spent fuel may eliminate a good deal of the need for extensive transmutation. It is, however, dependent on the content of the non-uranium spent nuclear fuel. It is advantageous to increase the proliferation resistance by not, for example, putting separated plutonium with an appreciable fissile fraction into the repository. However, if most of the weapons-usable material has been transmuted, then it is beneficial to remove the uranium from the fission products and other actinides. ^{238}U is, after all, basically natural uranium, and needn't take up extremely valuable room in the repository.

Volume Reduction

First, trials using 10 MONJU-sized fast reactors with the depleted uranium blanket/standard 16% RG-Pu MOX inner core/70% MA outer core loading were performed for various numbers of PWR's to see how many PWR cores would need to be converted to 1/3 MOX fueled thermal transmutation systems to get the spent fuel inventory below the statutory Yucca Mountain limit. These results are shown in Fig. 32.

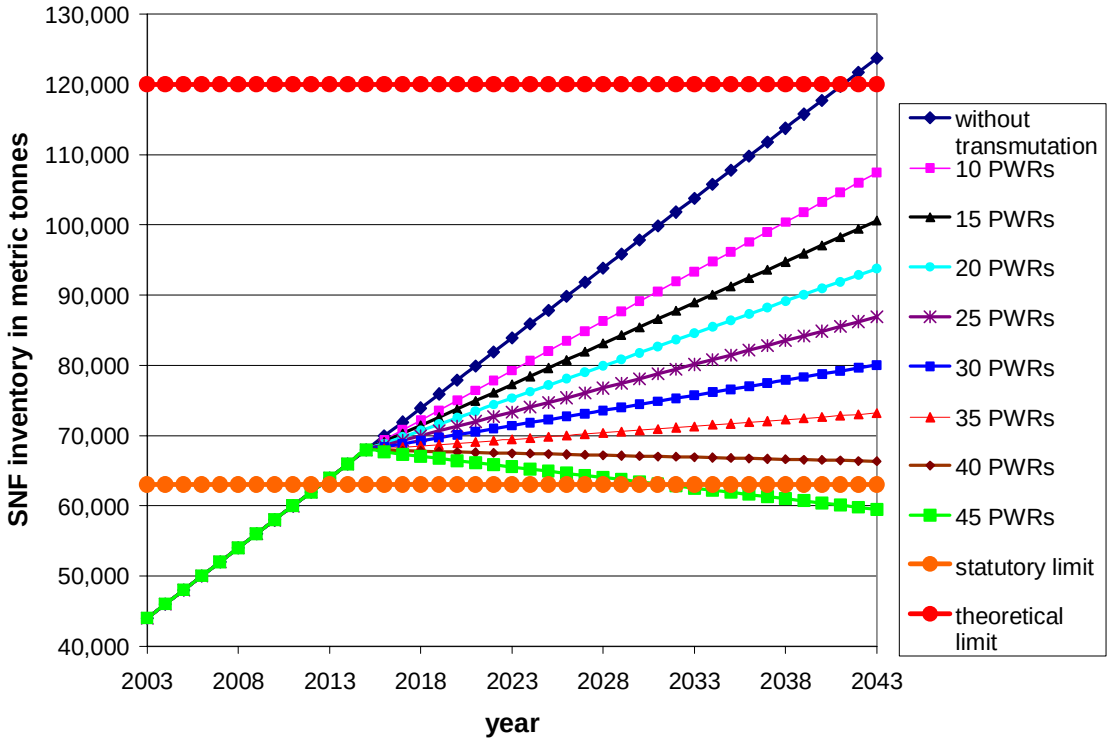

Fig. 32. Spent nuclear fuel inventory with 10 MONJU transmuters over 40 years.

These results are excellent, indicating that the total spent fuel inventory can be reduced to the levels indicated over a 40 year period. However, a number of assumptions have been made, as stated above. The largest one is that the transmutation core fuels will come entirely from the legacy spent fuel stockpile and not introduce any new material. This is cannot be correct, because the spent fuel stockpile doesn't contain enriched uranium and the non-MOX part of the transmutation cores is fresh 4% enriched uranium dioxide fuel. Although from a repository standpoint it would be advantageous to re-enrich the stockpile uranium, this will never happen economically. The other major assumption is that by 2015, all the reactors for transmutation will be built and online. Notice the lines are straight and begin diverging at 2015. It is more likely that

the curve will be a smooth curve as shown in Fig. 31, but for an approximation this presents a rough approximation.

If only 5 MONJU transmuters are built, the results look almost exactly the same over a 40 year period. While this seems incorrect, it is important to remember that these are total amounts of spent nuclear fuel. Fig. 33 and Fig. 34 display the difference in isotopic concentrations of spent fuel with different numbers of MONJU reactors, assuming 45 PWRs converted to MOX/plutonium transmutation. Fig. 33 uses a "low-MA" MONJU core loading, i.e., only the outer core is replaced with MA-bearing fuel. In the "high-MA" case, both the inner and outer core regions have MA-bearing fuels.

This is a very interesting chart, and it complicates the issue even further. For example, there cannot be negative amounts of spent fuel in the spent nuclear fuel stockpile. This reflects the input material that is necessary to make the proposed fuel cycle operate with the number of reactors indicated.

The thorium (not shown) is not a problem: one of the reasons thorium was chosen as the fertile diluent was its relative abundance. However, some of the other negative materials in Fig. 33 necessary to make the proposed cycle operate as indicated are more difficult to obtain. For example, largest drain is on the reserve of ^{239}Pu, and the need for 1,200 metric tonnes of ^{239}Pu is quite ironic, since this cycle is designed to burn plutonium as well as minor actinides.

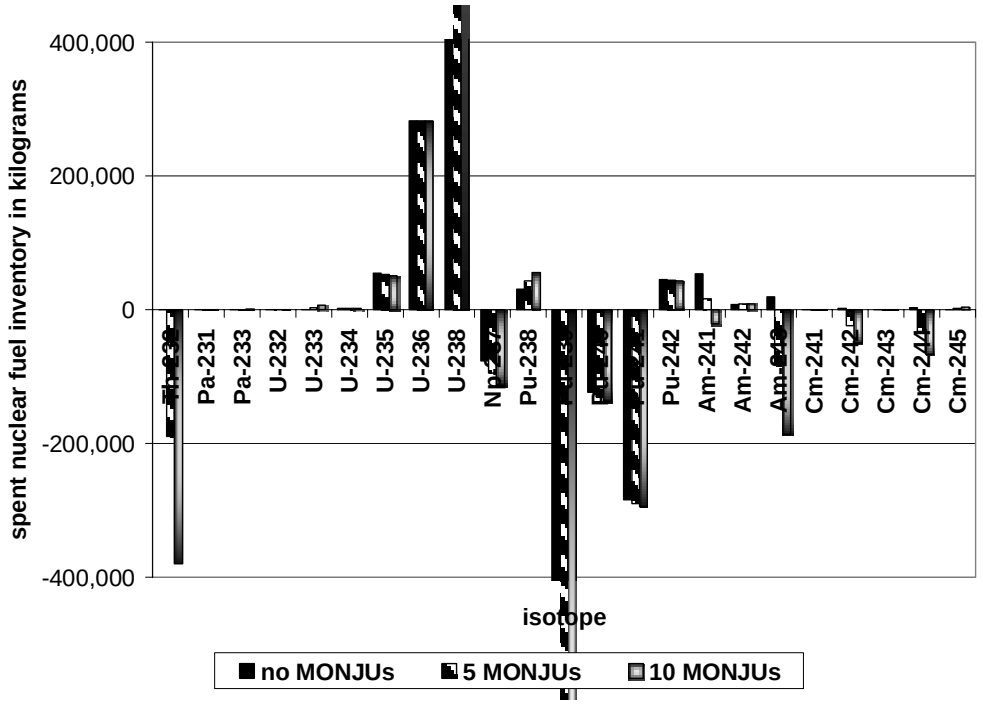

Fig. 33. Kilograms of spent fuel left after 40 years of transmutation with 45 transmutation PWRs and 0, 5, or 10 MONJU fast reactor transmutation systems.

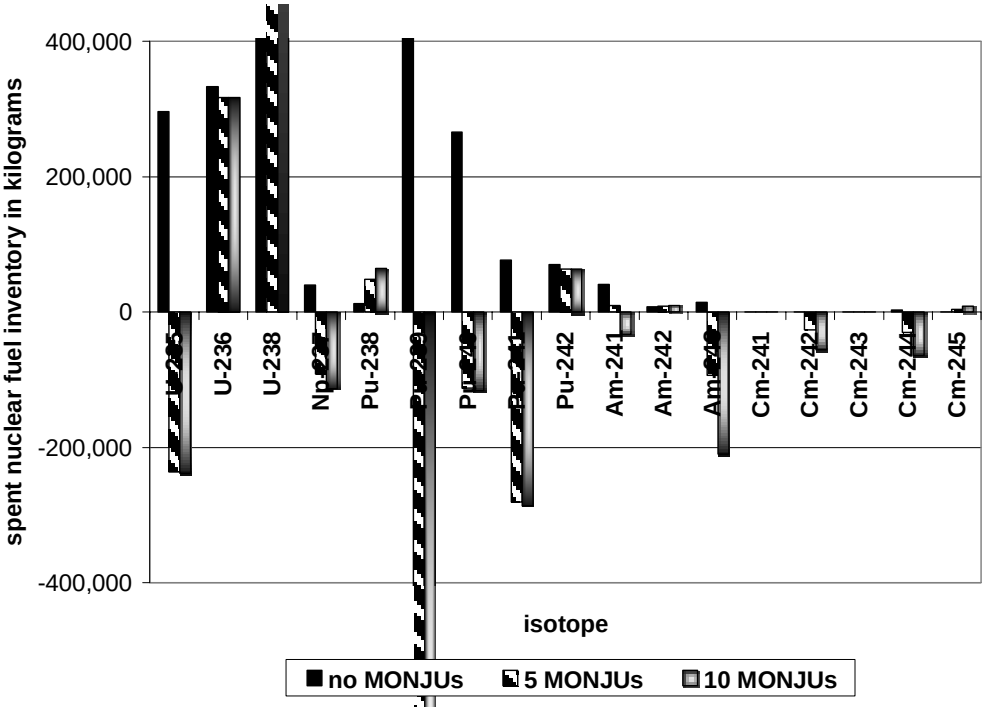

Fig. 34. Same as above, with "high-MA" MONJU core loading.

The fact that all the minor actinide values in Fig. 33 are negative is positive. Even 5 MONJU transmuter reactors the minor actinides will be eliminated from the spent nuclear fuel inventory and then some. However, the requirement for essentially weapons-grade plutonium is not quite such a positive result. The main advantage of these reprocessing schemes is the transmutation of neptunium, plutonium and the minor actinides, which these systems do quite well.

There are three main concerns for putting spent nuclear fuel into the Yucca Mountain Repository, all of which are interrelated as functions of the isotopic composition of the spent fuel. These concerns are the total volume of spent nuclear fuel destined for the repository, the long-term radiotoxicity of the repository's spent fuel, and the heat load of the spent fuel in the repository. The first concern is the volume of spent nuclear fuel that will need to be put into the repository, as shown above in Fig. 31 and Fig.32. A calculation of the current (as of 2003) spent nuclear fuel inventory by isotope is given in Fig. 35, and the isotopic composition after 10 years of transmutation with 40 MOX PWRs and 10 MONJU fast transmuters is given in Fig. 36.

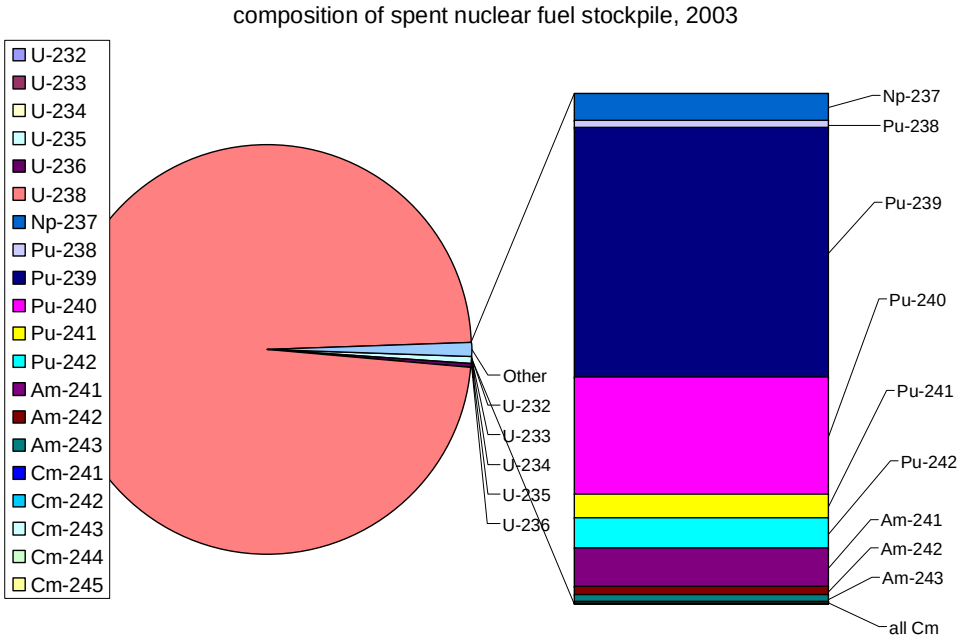

Fig. 35. Graphical representation of legacy spent nuclear fuel stockpile by isotope, 2003.

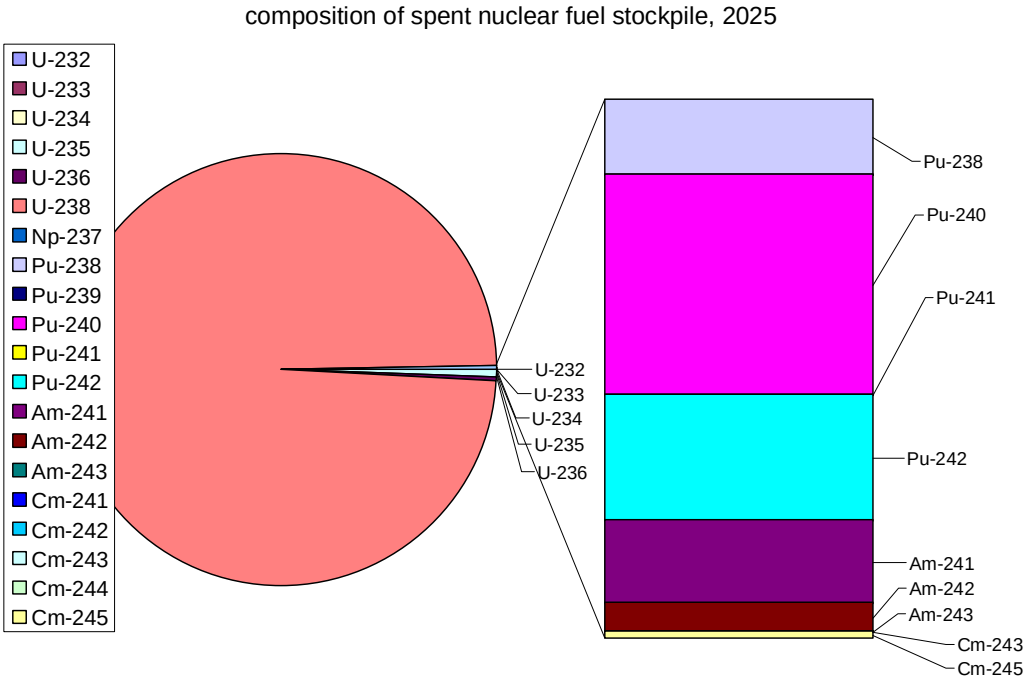

Fig. 36. Projection of the possible spent nuclear fuel stockpile after 10 years of transmutation.

These plots mainly serve to show the trend of the plutonium and minor actinide concentrations during burnup. The fissile ^{239}Pu, ^{241}Pu, and ^{241}Am decrease the most (in fact, there is a deficit of these isotopes with 40 PWR's and 10 MONJU cores), and the composition of the curium changes a great deal as well. The ^{242}Cm alpha decays with a half-life of ~162 days to produce ^{238}Pu. ^{242}Cm also has a large (n,γ) cross section, which produces ^{243}Cm. The ^{244}Cm has comparable reactions to produce ^{240}Pu and ^{245}Cm, except the half-life is 18 years.

The relative non-uranium fraction, however, stayed fairly constant. The two ways of dealing with the total volume of spent fuel are to reduce its absolute amount, and to reprocess it and separate out the depleted uranium. The majority of the spent nuclear fuel inventory is still uranium, particularly ^{238}U, and therefore some effort should be put into the separation at least some of the uranium from the other materials before the spent fuel is put into the repository. This is an easy way to reduce the total volume of spent fuel and depleted uranium is less radioactive than even natural uranium and it is therefore easier and less expensive to dispose of than high level waste. There are proliferation concerns, particularly dependent on the plutonium isotopes that are left in the high level waste and what form the waste is in. As can be seen in Fig. 36, however, there is no fissile plutonium left in the mixture, and indeed to run this many transmuter reactors additional fissile plutonium would be required as fuel.

Repository Heat Load

The heat generated by spent nuclear fuel is perhaps the biggest problem for the loading of the repository. Forsberg, one of the main proponents for separate disposal of

heat –generating spent nuclear fuel waste, in 2000 stated that "If there were no radioactive decay heat, the entire volume [of spent nuclear fuel in Yucca Mountain] could be placed in a cube, which would be ~30 m on a side." The Yucca Mountain Repository has many miles of tunnels, and one reason for this is to limit the temperature of the waste. Clearly, the heat generated by the spent nuclear fuel in the repository is the biggest limiting factor to the amount of waste that can be safely stored there [31].

The specific heat loads of various isotopes of interest were calculated with ORIGEN2 and are given in Table 15. Some of these isotopes were not tracked in Monteburns, and that is because even though they have large specific heat loads, they have very short half-lives and decay rapidly.

Table 15
Specific heat loads of some important isotopes, calculated with ORIGEN2.

Isotope	Half-life, years	Specific Heat Load, W/kg
U235	7.04E+08	5.66E-05
U237	1.85E-02	1.54E+05
U238	4.47E+09	8.53E-06
U239	4.46E-05	9.01E+07
NP237	2.14E+06	2.10E-03
NP238	5.79E-03	1.24E+06
NP239	6.45E-03	5.61E+05
NP240	1.18E-04	1.28E+08
PU238	8.77E+01	5.68E+02
PU239	2.41E+04	1.92E+00
PU240	6.56E+03	7.10E+00
PU241	1.40E+01	3.20E+00
PU243	3.75E+05	3.01E+06
AM241	4.33E+02	1.14E+02
AM243	7.37E+03	6.41E+00
CM242	4.46E-01	1.22E+05
CM243	2.91E+01	1.89E+03
CM244	1.81E+01	2.83E+03
CM245	8.50E+03	5.70E+00

A good example of this is ^{237}U, which has a specific heat load of 154 kilowatts per kilogram, but a half-life of less than a week (6.75 days). This decays to ^{237}Np, which has a specific heat load of only 0.021 watts per kilogram. These isotopes that were omitted from the calculations are more of an issue for spent fuel pool designers than for determining the long term heat load for a repository.

The heat load for one metric tonne of legacy spent fuel without fast reactor transmutation is compared with that of one metric tonne spent nuclear fuel with the transmutation compositions shown in Fig. 37. These values reflect the heat generation at discharge from the fuel cycle.

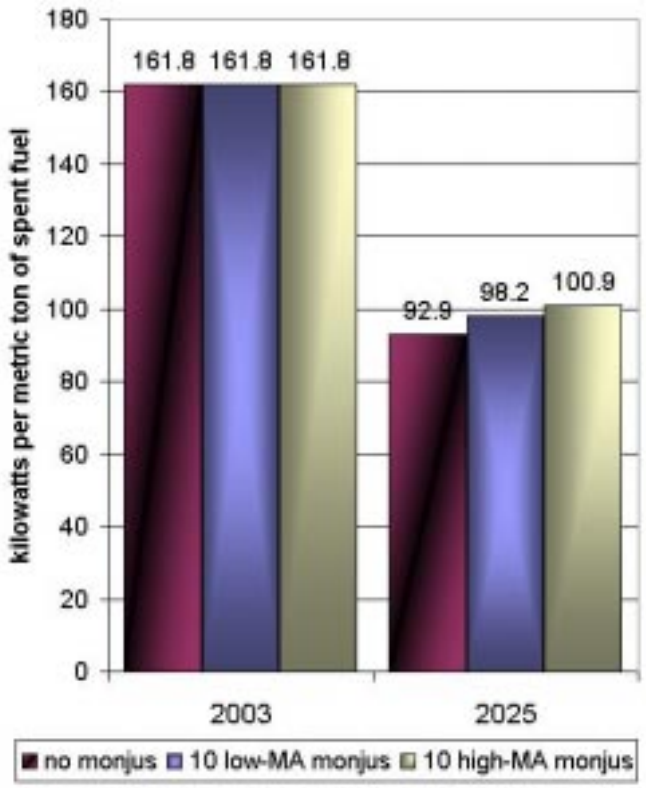

Fig. 37. Relative change in the heat generation rate per metric ton of spent fuel from the actinides due to transmutation.

The advantage gained from transmutation is quite large; the heat generation rate per unit of spent fuel (kW per MT or W per kg) from the actinide elements has been reduced over 40%, which will have a major impact on the repository. The heat generated by the high-MA fueled core is actually a bit higher at discharge compared to transmutation without MONJU reactors. This changes over the long term, however. In addition to the actinide isotopes listed in Table 15, the fission products ^{137}Cs and ^{90}Sr (among others) have a large impact in the first few hundred years or so of storage in the repository (each of these isotopes has a half-life of around 30 years), but after this initial period the long-lived isotopes of Pu, Am and Cm dominate. Fig. 38 shows the decay of spent fuel from the 30% MA inner core, 60% MA outer core MONJU cycle.

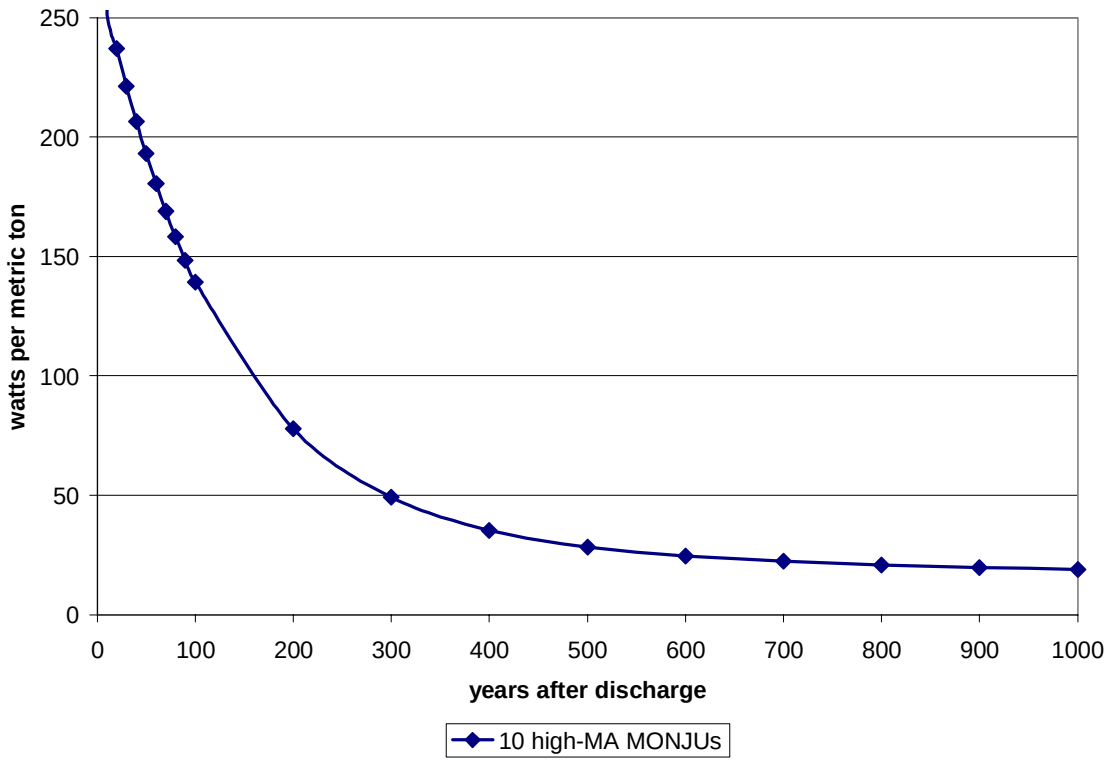

Fig. 38. Impact of short-term high-heat generating actinides on heat load.

As can be seen in Fig. 38, the heat generated in the fuel drops dramatically in the first ten years, and from 10 years to 100 years decreases another 55%. The impact of using more MONJU transmuters and different core loadings in those systems can be seen more clearly in Fig. 39. Using ORIGEN2, the spent fuels from the transmutation scheme indicated after 10 years of transmutation were allowed to decay for 1,000 years. The term "high-MA fuels" refers to the MONJU core loading consisting of a depleted uranium blanket, 30% MA fuel in the inner core and 60% MA in the outer core. In contrast, "low-MA fuels" refers to a depleted uranium blanket, 16% RG-Pu MOX fuel in the inner core and 60% MA in the outer core.

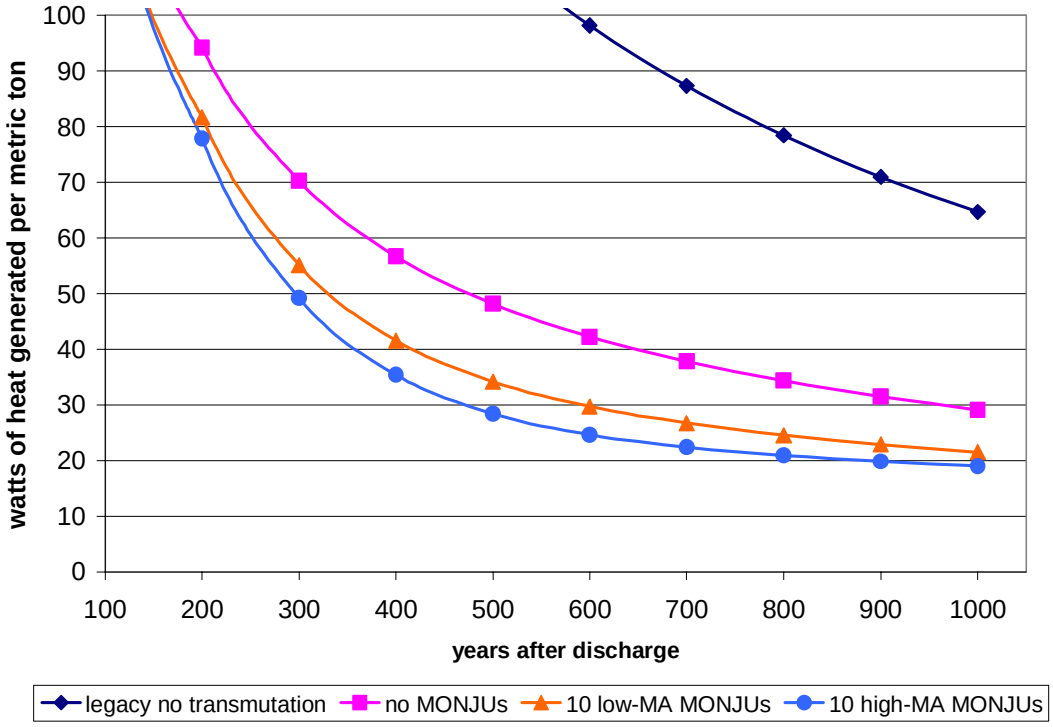

Fig. 39. Long-term heat load with and without fast transmutation.

Thus, adding a fast transmutation system, or adding more minor actinides to that transmutation system creates a large reduction in heat load. By implementing fast transmutation systems, the heat load per metric ton is reduced almost one-quarter by using the low-MA fuels and over one-third by using the higher-MA loading from the value calculated with only thermal transmutation.

The main problem in the long term with the proposed recycle strategy will be balancing the needs of the transmuter reactors to the amount of legacy spent fuel from the commercial nuclear power industry. The models generated in this chapter are intended to give a general idea of the complexity of the closed fuel cycle, and an estimate for the transmutation strategy that would be most beneficial.

Radiotoxicity Effects

The other reason for a large reduction in the neptunium, plutonium and minor actinides in the spent nuclear fuel inventory is that these nuclides provide the most radiation in the long term. Most of these nuclides have substantially long half-lives and are quite radioactive, as can be seen in Table 16. Their specific radioactivities were calculated with ORIGEN2.

The spent fuel compositions from the transmutation cycles using high-MA MONJU cores, low-MA MONJU cores, no MONJUs, and no transmutation at all are given in Fig. 40. These values follow the same trend as the heat load, which is not surprising since most of the nuclides with longer half-lives have smaller specific heat loads, as shown in the data in Table 15.

Table 16
Radioactivities and half-lives of some important nuclides, sorted by half-life

Isotope	Half-life, years	Radioactivity, Curies per kilogram
U-238	4.47E+09	3.36E-04
U-235	7.04E+08	2.16E-03
Cm-247	1.56E+07	9.28E-02
Np-237	2.14E+06	7.05E-01
Pu-243	3.75E+05	2.60E+10
Cm-248	3.48E+05	4.25E+00
U-233	1.59E+05	9.68E+00
Pa-231	3.28E+04	4.73E+01
Pu-239	2.41E+04	6.22E+01
Cm-245	8.50E+03	1.72E+02
Am-243	7.37E+03	1.99E+02
Pu-240	6.56E+03	2.28E+02
Cm-246	4.76E+03	3.07E+02
Am-242	1.14E+03	8.09E+08
Am-241	4.33E+02	3.43E+03
Pu-238	8.77E+01	1.71E+04
Cm-243	2.91E+01	5.16E+04
Cm-244	1.81E+01	8.09E+04
Pu-241	1.40E+01	1.03E+05

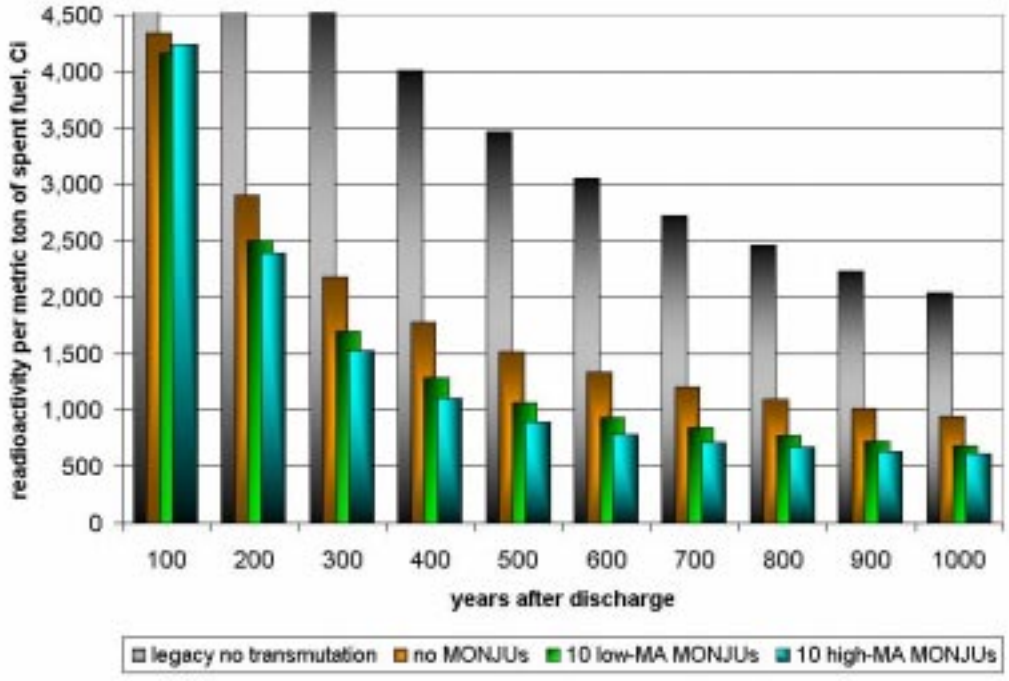

Fig. 40. Radioactivity of spent nuclear fuel in curies, one metric tonne over 1,000 years.

As shown in Fig. 40, the difference between thermal transmutation only and by adding just 10 MA-fueled MONJU reactors is quite large. The long-term radioactivity can be reduced by as much as 54% with just 10 years of transmutation in thermal systems alone. By adding the second tier fast transmutation systems, the reduction in long-term radioactivity climbs over 70%.

Chapter Summary

In this chapter the immense task of closing the fuel cycle was undertaken. The most difficult part of trying to balance the production and burn of spent nuclear fuel in the transmutation fuel cycle is choosing the variables. There are many variables that need to be taken into account and almost all of them are subject to change. For example, the approximations made in doing these calculations are quite significant. These include assuming that all US power reactors are PWRs of the 3411 MWth Westinghouse 17x17 design, all will continue running for the full duration modeled, all the transmutation systems built into the model will come online at the same time, and that it will be economically possible to implement these factors. Smaller issues with large impacts, such as license extensions for existing plants, were not and can not be accounted for at this time. In the end, all of these important decisions will have to be made, and all variables accounted for. For now, some of these important questions were answered by pure conjecture. The goal of this study was to find at least one possible solution to transmuting spent nuclear fuel and closing the fuel cycle.

That being said, it was shown that, within the scope of this study, effective reductions in the total volume of spent nuclear fuel, the radioactivity of that fuel and the

repository heat load of the spent nuclear fuel inventory can be made by a two-tier transmutation scheme involving the conversion of up to 45 PWR reactors to burn 0.04% Np / 7.6% Pu MOX fuels in a 1/3 core loading, and the building of up to 10 MONJU-size fast reactor systems to be loaded with either of two compositions of minor-actinide bearing thorium nitride transmutation fuels.

CHAPTER V

SUMMARY AND CONCLUSIONS

This study was conducted under funding from the Advanced Fuel Cycle Initiative. The purpose was to investigate reducing the spent nuclear fuel inventory to prevent the overloading of the Yucca Mountain Repository and to decrease the need for a second repository in the future. A two-tier reprocessing and transmutation strategy has been proposed by the Department of Energy, and followed in this study. The thermal-spectrum transmutation of plutonium and neptunium using the existing fleet of US power reactors with slightly modified mixed oxide (MOX) fuels is designated Series I. Series II consists of the use of as-yet unbuilt fast-spectrum reactors to transmute the minor actinides that are of concern due to their long half-lives, high radioactivity and high heat-generation rates.

First, a Westinghouse PWR design was chosen for the Series I thermal spectrum transmuter and calculations were performed for various different MOX fuels. Single fuel pins were modeled in an infinite lattice to determine their relative transmutation rates and k_{inf} values. The best transmutation MOX fuel was determined to be 7.6% reactor-grade (RG) plutonium, 0.04% neptunium, and the balance was made up with depleted uranium (99.3% ^{238}U). The k_{eff} values for this fuel were within the range calculated without the addition of neptunium to the MOX, and although control rods and soluble boron were added to the model, these control features were not modified over the reactor cycle as they would be in a real plant. The results indicate that thermal

transmutation in existing light-water reactor systems reduces the fissile plutonium inventory, but builds in a small amount of the non-fissile plutonium isotopes as well as some minor actinides.

Next, the design for the Japanese sodium-cooled fast reactor MONJU was chosen as the fast-spectrum Series II transmuter. Various fuels were modeled, again first as single pins in an infinite lattice. The higher minor actinide (MA) concentrations transmuted more of the minor actinides they contained, but were very reactive, whereas the lower MA-containing fuels more closely resembled the MOX fuels that are standard to the MONJU core. When these fuels were put into the whole core model, two different core loadings were considered after many factors such as the amount of minor actinides available for fabricating these fuels were taken into account. The best designs consisted of keeping the depleted uranium blanket region of MONJU intact. The inner and outer core loadings that gave the best results consisted of using either 30% MA and 60% MA fuels, or standard MOX and 70% MA fuels, respectively. The transmutation of the minor actinides, despite some buildup of ^{238}Pu, demonstrated the advantage of a fast reactor system for this stage of transmutation.

To close the fuel cycle, various numbers of PWRs were converted to Series I transmutation systems and coupled with different numbers of MONJU Series II systems. The target starting date for transmutation was set at 2015, which is perhaps ambitious. Calculations were performed to determine the volume of spent nuclear fuel after adopting this strategy, the radioactivity of the spent fuel remaining and its heat generation rate from discharge to 1,000 years. The implementation of spent nuclear fuel

reprocessing and transmutation in a two-tier system was shown to greatly reduce these three parameters which present the largest problems for the repository.

There are many factors beyond the scope of this study that were not addressed. For example, the only safety-related reactor physics parameter investigated for these fuels and transmutation systems was the delayed neutron fraction. In addition, the MONJU reactor design used as the fast transmutation system is a very good design, but any new reactor built in the US will likely be of a design developed under the Generation IV reactor program. Several of the proposed Generation IV reactors will have fast or epithermal spectrums which could serve the same role as the MONJU core used in this study to burn the majority of the minor actinides in spent fuel. Obviously, these reactors will have different transmutation capacities than MONJU with the proposed layouts, but the end result should be the same. The spent nuclear fuel inventory can be reduced and the fuel cycle closed through careful management and planning.

REFERENCES

[1] A Roadmap for Developing ATW Technology: A Report to Congress, US DOE/RW- 0519, October 1999.

[2] AFCI Quarterly Report, January-March 2003, SAND2003-2060P, June 2003.

[3] H.W. Weise, J. Alloys Comp. 271-273 (1998) 522.

[4] M. Todosow, LWR physics analyses, Np+Pu assembly designs, reduced water moderated reactor, in: AFCI Semi-Annual Review Meeting, Santa Fe, NM, August 26-28, 2003.

[5] K.Nikitin, M. Saito, M. Kawashima, V. Artisyuk, A. Shmelev, J. Nucl. Sci. and Tech. 38, no.7, (July 2001) 511.

[6] K. Pasamehmetoglu. AFCI fuels development, in: AFCI Semi-Annual Meeting, Albuquerque, NM, January 22-23, 2003)

[7] K. Kurosaki, K. Yano, K. Yamada, M. Uno, S. Yamanaka, J. Alloys Comp. 319 (2001) 253-257.

[8] Y. Suzuki, T. Ogawa, T. Osugi, Y. Arai, T. Mukaiyama, Research and development of nitride fuel cycle for TRU burning, in: Proceedings of the Fourth International Information Exchange Meeting on Actinide and Fission Product Partitioning and Transmutation, Mito City, Japan, September 11-13, 1996.

[9] J. Wallenius, CONFIRM: Collaboration on nitride fuel irradiation and modeling, in: Proceedings of Nuclear Applications in the New Millenium (AccAPP-ADTTA'01), Reno, Nevada, November 11-15, 2001.)

[10] J. Wallenius and S. Pillon. N-15 requirement for 2nd stratum ADS nitride fuels, in: Proceedings of Nuclear Applications in the New Millenium (AccAPP-ADTTA'01), Reno, Nevada, November 11-15, 2001.

[11] I. Yu. Krivitski, M.F. Vorotyntsev, V.K. Pyshin, L.V. Korobeinikova, Prog. Nucl. Energy. 38, No. 3-4 (2001) 391.

[12] C. Lombardi, A. Mazzola, E. Padovani, and M.E. Ricotti, J. Nucl. Mater. 274 (1999) 181.

[13] C.W. Forsberg, C.M. Hopper, J.L. Richter, H.C. Vantine, Definition of weapons-usable uranium-233, Oak Ridge National Laboratory document ORNL/TM-13517, March 1998.

[14] M.B. Davis, *La France Nucleaire*: http://www.francenuc.org/en_mat/uranium3_e.htm, accessed on 1/27/2004.

[15] Thorium, Uranium Information Centre Briefing Paper #6, November 2003 http://www.uic.com.au/nip67.htm

[16] M.S. Kazimi, *Thorium Fuel for Nuclear Energy*. American Scientist 91 5 (September-October 2003), 408-413.

[17] X5 Monte Carlo Team, MCNP-A General Monte-Carlo N-Particle transport code, version 5, Los Alamos National Laboratory document LA-UR-03-1987, April 2003.

[18] A.G. Croff, A user's manual for ORIGEN2 computer code, Oak Ridge National Laboratory document ORNL/TM-7175, July 1980.

[19] S.B. Ludwig, A.G. Croff to J. Manneschimdt, memorandum regarding Version 2.2

update to ORIGEN2 computer code, May 23, 2002.

[20] H. Trellue, D. Poston, User's manual, version 2.0 for Monteburns, version 5B, Los Alamos National Laboratory document LA-UR-99-4999, September 1999.

[21] W.S. Charlton, R.T. Perry, B.L. Fearey, T.A. Parish, Nucl. Tech. 131 (2) (2000) 210.

[22] N.E. Todreas, M.S. Kazimi, Nuclear Systems I, Taylor and Francis, New York, 1993.

[23] MONJU, Technical Data. http://www.jnc.go.jp/zmonju/mjweb/technical.htm, accessed 1/29/2004.

[24] Hiroshi Nishi, private communication.

[25] W.M. Stacey, Nuclear Reactor Physics, John Wiley and Sons, New York, 2001.

[26] H.R. Trellue, Reduction of the radiotoxicity of spent nuclear fuel using a two-tiered system comprising light water reactors and accelerator-driven systems, doctoral dissertation, University of New Mexico, Department of Nuclear Engineering, 2003.

[27] S.M.A. Reynaud, Nitride fuel performance, Master's thesis, Texas A&M University, Department of Nuclear Engineering, May 2002.

[28] Y. Arai, K. Nakajima, Y. Suzuki, J. Alloys Comp. 271-273 (1998) 602.

[29] R. Thetford, M. Mignanelli, J. Nucl. Mat. 320 (2003) 44.

[30] W.S. Charlton, The Nuclear Fuel Cycle, lecture given as part of NUEN 689, Texas A&M University, Department of Nuclear Engineering, Spring 2004.

[31] C.W. Forsberg, Disposal of partitioning-transmutation waste with separate

management of high heat radionuclides, in: Proceedings of the 6th Information Exchange Meeting on Actinide and Fission Product Partitioning and Transmutation, 11-13 December 2000, Madrid Spain

[32] J. Herczeg, LWR physics analyses, Np+Pu assembly designs, reduced water moderated reactor, in: AFCI Semi-Annual Review Meeting, Albuquerque, NM, January 22-24, 2003.

[33] M. Brady, Evaluation and application of delayed neutron precursor data, doctoral dissertation, Texas A&M University, Department of Nuclear Engineering, December 1988.

APPENDIX A

DELAYED NEUTRON DATA

This data was used to calculate the delayed neutron fractions of the various fuels modeled in this study, according to the method outlined in Chapter 2. They were taken from a doctoral thesis by Michaele Brady [33].

Table A.1
Comparison of Total Delayed Neutron Yield per 100 Fissions

Isotope	ν_d^j
Th-232	5.64
Pa-231	1.6
Pa-233	not available
U-232	0.52
U-233	0.9
U-234	1.29
U-235	2.06
U-236	2.32
U-238	4.05
Np-237	1.14
Pu-238	0.79
Pu-239	0.68
Pu-240	0.51
Pu-241	1.42
Pu-242	1.43
Am-241	0.51
Am-242	0.78
Am-243	0.8
Cm-241	not available
Cm-242	0.14
Cm-243	not available
Cm-244	not available
Cm-245	0.64
Cm-246	not available
Cm-247	not available
Cm-248	not available

Table A.1
Continued

Cf-249	0.16
Cf-251	0.75

Table A.2
Delayed neutron six-group parameters

	Group					
Isotope	1	2	3	4	5	6
Th-232	0.0364	0.1259	0.1501	0.4406	0.1663	0.0808
Pa-231	0.0826	0.223	0.1608	0.3885	0.105	0.0401
Pa-233	n/a	n/a	n/a	n/a	n/a	n/a
U-232	0.136	0.2745	0.1509	0.3052	0.1007	0.0326
U-233	0.0859	0.2292	0.1781	0.3516	0.1142	0.0409
U-234	0.055	0.1964	0.1803	0.3877	0.1324	0.0482
U-235	0.035	0.1807	0.1725	0.3868	0.1586	0.0664
U-236	0.0302	0.1722	0.1619	0.3841	0.1775	0.0741
U-238	0.0139	0.1128	0.131	0.3851	0.254	0.1031
Np-237	0.04	0.2162	0.1558	0.3633	0.1659	0.0589
Pu-238	0.0377	0.239	0.1577	0.3562	0.159	0.0504
Pu-239	0.0363	0.2364	0.1789	0.3267	0.1702	0.0515
Pu-240	0.032	0.2529	0.1508	0.3301	0.1795	0.0547
Pu-241	0.018	0.2243	0.1426	0.3493	0.1976	0.0682
Pu-242	0.0196	0.2314	0.1256	0.3262	0.2255	0.0716
Am-241	0.0355	0.254	0.1563	0.3364	0.1724	0.0454
Am-242	0.0247	0.2659	0.1512	0.3337	0.1756	0.0489
Am-243	0.0234	0.2945	0.1537	0.3148	0.1656	0.048
Cm-241	n/a	n/a	n/a	n/a	n/a	n/a
Cm-242	0.0763	0.2847	0.1419	0.2833	0.1763	0.0375
Cm-243	n/a	n/a	n/a	n/a	n/a	n/a
Cm-244	n/a	n/a	n/a	n/a	n/a	n/a
Cm-245	0.0222	0.1788	0.1672	0.3706	0.2054	0.0559
Cm-246	n/a	n/a	n/a	n/a	n/a	n/a
Cm-247	n/a	n/a	n/a	n/a	n/a	n/a
Cm-248	n/a	n/a	n/a	n/a	n/a	n/a
Cf-249	0.0246	0.3919	0.1349	0.2598	0.1614	0.0273
Cf-251	0.0055	0.3587	0.1736	0.2693	0.1688	0.0242

APPENDIX B

MONJU SPECIFICATIONS

This data was originally all taken from the MONJU website which is very interesting and informative. However, a special mention of and some special thanks to Dr. Hiroshi Nishi at JNC who sent me the data before it was published on the web, and translated it from Japanese for me [23,24]. In addition, there was some extra materials data unavailable on the website which Dr. Nishi gave to me and can be found in Tables B.4 and B.5.

Table B.1
Major specifications of MONJU core, including fuel subassembly

Core Fuel Pellet	units	
Material		MOX and Uranium Dioxide
Plutonium Isotopic Composition (^{238}Pu, ^{239}Pu, ^{240}Pu, ^{241}Pu, ^{242}Pu)	wt%	0/58/24/14/4
Pu-Fissile* Enrichment, Inner Core / Outer Core *(^{239}Pu+ ^{241}Pu)	%	14.4/19.9
Uranium Isotopic Composition (^{235}U/^{238}U)	wt%	0.2/99.8
Fuel Stack Height	mm	930
Outer Diameter	mm	5.40
Percent of Theoretical Density	%	85
Stoichiometry (O/M)		1.97
Axial Blanket Fuel Pellet		
Material		Uranium Dioxide
Uranium Isotopic Composition U235/U238	wt%	0.2/99.8
Fuel Stack Height		
Upper Blanket	mm	300
Lower Blanket	mm	350
Outer Diameter	mm	5.40

Table B.1 Continued		
Percent of Theoretical Density	%	93
Stoichiometry (O/M)		2.00
Cladding Tube	**units**	
Material		SUS316 Equivalent Stainless Steel
Outer Diameter	mm	6.50
Inner Diameter	mm	5.56
Thickness	mm	0.47
Spacer Wire		
Material		SUS316 Equivalent Stainless Steel
Outer Diameter	mm	1.32
Wire Wrapping Pitch	mm	307
Fuel Subassembly		
Array of Pins		Equilateral Triangular Lattice
Pin Pitch	mm	7.87
Number of Pins per subassembly		169
Subassembly Pitch	mm	115.6
Subassembly Wrapper Tube		
Material		SUS316 Equivalent Stainless Steel
Outer Flat-to-Flat Distance	mm	110.6
Inner Flat-to-Flat Distance	mm	104.6
Thickness	mm	3.0

Table B.2.
Major specifications of MONJU blanket, including fuel subassembly

Blanket Fuel Pellet	units	
Material		Uranium Dioxide
Uranium Isotopic Composition		
U235/U238	wt%	0. 2/99.8
Fuel Stack Height	mm	1580
Outer Diameter	mm	10.40
Percent of Theoretical Density	%	93
Stoichiometry (O/M)		2.00
Wrapper Tube		
Material		SUS316 Equivalent Stainless Steel

Table B. 2
Continued

Outer Diameter	mm	11.60
Inner Diameter	mm	10.60
Radial Thickness	mm	0.50
Spacer Wire		
Material		SUS316 Equivalent Stainless Steel
Outer Diameter	mm	1.50 （0.9: only for the outermost pins）
Wire Wrapping Pitch	mm	251.0
Fuel Subassembly		
Array of Pins		Equilateral Triangular Lattice Array
Pin Pitch	mm	13.15
Number of Pins		61
Subassembly Pitch	mm	115.6
Subassembly Wrapper Tube		
Material		SUS316 Equivalent Stainless Steel
Outer Flat-to-Flat Distance	mm	110.6
Inner Flat-to-Flat Distance	mm	104.6
Thickness	mm	3.0

Table B.3
MONJU control rod characteristics

Fine Control Rod		
Material of Neutron Absorber		B_4C
^{10}B Enrichment	wt%)	39
Percent of Theoretical Density of B_4C-Pellet	%	95 *1）
B_4C-Pellet Outer Diameter	mm	12.2
Cladding Tube Outer/Inner Diameter	mm	16.9/12.9
Number of Absorber Pins		19
Absorber Stack Height	mm	800
Material of Cladding Tube		SUS316 Equivalent Stainless Steel
Coarse Control Rod		
Material of Neutron Absorber		B_4C
^{10}B Enrichment	wt%	39

Table B.3
Continued

Percent of Theoretical Density of B4C-Pellet	%	95 *1)
B4C-Pellet Outer Diameter	mm	12.2
Cladding Tube Outer/Inner Diameter	mm	16.9/12.9
Number of Absorber Pins		19
Coarse Control Rod		
Absorber Stack Height	mm	800
Material of Cladding Tube		SUS316 Equivalent Stainless Steel
Back-up Control Rod		
Material of Neutron Absorber		B_4C
^{10}B Enrichment	wt%	90
Percent of Theoretical Density of B4C-Pellet	%	95 *1)
B4C-Pellet Outer Diameter	mm	14.2
Cladding Tube Outer/Inner Diameter	mm	16.9/14.9
Number of Absorber Pins		19
Absorber Stack Height	mm	930
Material of Cladding Tube		SUS316 Equivalent Stainless Steel
Shielding Subassembly		
Number of Subassemblies		2580
Height	mm	316
Neutron Shield (Cylinder Block in Wrapper Tube） Outer Diameter	mm	
Wrapper Tube		100 *1)
Inner Flat-to-Flat Distance	mm	104.6
Outer Flat-to-Flat Distance	mm	110.6
Material of Wrapper Tube/Shield		SUS316 Equivalent Stainless Steel

Table B.4
MONJU materials properties, density

Core Materials	Specific Material	Density (g/cm^3)
Fuel	MOX	11.08（Pu Enrichment for 20wt%）
	UO_2	10.96
Structural Materials	SUS316	7.97
	SUS304	7.90
Coolant	Na	Rho =0.9500-2.298×10^{-4}T-1.461×$10^{-8}$$T^2$＋5.638×$10^{-12}$$T^3$ Rho：Density of Coolant（g/cm^3） T：Temperature of Coolant（℃）
Absorber	B_4C	2.49

Table B.5
MONJU materials properties, temperature

Core	Region	Temperature（K）
Initial Critical Core	Whole Core	473
Initial Start-up Core (BOC at rated power)	Inner Core	1431
	Outer Core	1331
	Axial Blanket	760
	Radial Blanket	729
	Others	673

VITA

Born in Syracuse, New York on May 13, 1980, Frank Joseph Szakaly, son of Frank and Karen Szakaly, attended high school in Baldwinsville, NY and graduated in 1998 with a focus on physics, history, and art. He later attended the University of Rochester in Rochester, NY, graduating in May of 2002. He earned two baccalaureate degrees while there, receiving a B.A. in physics and a B.A. in European history, and a minor in English Literature. He then came to Texas A&M University in the fall of 2002 to pursue a master's degree in Nuclear Engineering.

Mr. Szakaly can be reached at 313 Delwood Drive, Baldwinsville NY 13027, and his permanent email address is frankszakaly@yahoo.com